Arab J Geosci (2017) 10: 351
DOI 10.1007/s12517-017-3134-6

ARABGU2016

Hoggar geochronology: a historical review of published isotopic data

Faten Bechiri-Benmerzoug [1,2] · **Bernard Bonin** [3] · **Hamid Bechiri** [2] · **Rékia Khéloui** [1,2] · **Sabiha Talmat-Bouzeguela** [1] · **Khadija Bouzid** [1]

Received: 30 March 2017 / Accepted: 24 July 2017 / Published online: 14 August 2017

Abstract A dataset of more than 400 isotopic ages on the Hoggar Shield, published from 1963 to 2017, was obtained by increasingly precise isotopic dating techniques and low-temperature thermochronology. Data were arranged by eras and terranes and classified in two categories "before 1980" and "after 1980". They illustrate the protracted geological history of the Hoggar Shield. The first continental *nuclei* were formed 3.5–2.5 Ga ago during the Archean, with high-grade metamorphic and associated magmatic episodes. A second group of continental terranes was created 2.40–1.75 Ga ago during the Paleoproterozoic, with Eburnean orogenic episodes marked by reworking of older Archean terranes associated with juvenile terranes. After the 1.80–0.90 Ga long period of quiescence, the 870–540 Ma Neoproterozoic times were characterized by Pan-African episodes, with early overthrusting of eclogitic nappes and late strike-slip movements along north-south trending shear zones, high-grade metamorphism and anatexis, emplacement of large granitoid batholiths followed by complexes of the Taourirt igneous suite. Cambrian hydrothermal activity evidences either a slow cooling process, or more likely discrete thermal pulses. After scarce Carboniferous mafic magmatism, the Mesozoic and the beginning of the Cenozoic constituted a period of quiescence marked by subsidence and burial after the Early Cretaceous. Low-temperature chronology records episodes of alternating subsidence and exhumation. Widespread Eocene exhumation predated volcanic activity beginning in the Late Eocene and continuing until recent times, in association with Africa–Europe convergence processes.

Keywords Isotopic dating techniques · Low-temperature thermochronology · Archean · Paleoproterozoic · Neoproterozoic · Paleozoic · Mesozoic · Cenozoic · High-grade, high-pressure, high-temperature metamorphisms · Granitoid batholiths · Taourirt igneous suite · Volcanic activity

This article is part of the Topical Collection on *Current Advances in Geology of North Africa*

✉ Faten Bechiri-Benmerzoug
faty_benmerzoug@yahoo.fr

Bernard Bonin
bernard.bonin@u-psud.fr

[1] Departement des Sciences Naturelles, École Normale Supérieure, B.P. No. 92, 16308 Vieux-Kouba, Alger, Algeria

[2] Laboratoire de Métallogénie et du Magmatisme de l'Algérie (LMMA), FSTGAT/USTHB, BP32, El Alia, 16111 Bab Ezzouar, Alger, Algeria

[3] "GEOPS", Université Paris-Sud, CNRS UMR8148, Université Paris-Saclay, Rue du Belvédère, F-91405 Orsay Cedex, France

Introduction

Sahara is the largest arid desert in the world. It is mostly composed of either flat, or mountainous areas, where geological formations and their mutual contacts are fairly well-exposed. All types of rocks occur, and their ages range from Archean to recent times. Within high-elevation zones, the Hoggar is the most prominent. It is made up of a large swell of Precambrian formations, decorated in the highs by impressive Neogene volcanic domes and peaks culminating at c. 3000 m above sea level. Precambrian formations at altitudes ranging from about 400 m up to 2500 m constitute the central part of the Tuareg Shield. Their boundaries are defined by unconformably overlying Lower Paleozoic Tassili formations.

The Archean–Proterozoic Tuareg shield is characterized by north-south trending major shear zones, which separate crustal blocks with contrasting geology. It is interpreted as an amalgamation of terranes (Black et al. 1994) that were welded between the West African Craton and the East Saharan Metacraton (Abdelsalam et al. 2002; Liégeois et al. 2013) during the 850–630 Ma Pan-African orogeny (e.g.Caby 2003; Liégeois et al. 2003; and references therein). This major event was achieved through episodes of dockings, or collisions, affecting continental blocks and of accretions of oceanic island arcs. It resulted into the welding of the northeastern part of West Gondwana. Subsequent strike-slip movements along mega-shear zones built the current shape of the shield. Eocene initiation of the Hoggar Swell (Rougier et al. 2013) and Cenozoic intraplate volcanic episodes (Liégeois et al. 2005) constitute the last geological events that have affected the Tuareg Shield.

In the central Sahara, the Hoggar or Ahaggar massif in southern Algeria, together with the Adrar of Iforas in northern Mali and Aïr in northern Niger, form the Tuareg Shield, displays variably deformed and metamorphosed sedimentary, volcanic and plutonic rocks that span from the Paleoarchean to the Latest Cenozoic (~3400 to ~1.51 Ma, Fig. 1). Precambrian rocks are currently organized in 16 terranes. Their boundaries correspond to lithospheric mega-shear zones, which favoured emplacement of postorogenic plutons of the "Taourirt" suite (Azzouni et al. 2003). Suture zones are often highlighted by the following: (a) mafic and ultramafic complexes interpreted as ophiolites; (b) eclogite (e.g., Zetoutou et al. 2004; Doukkari et al. 2014, 2015; Berger et al. 2014) and whiteschist slices (e.g., Adjerid et al. 2015); (c) TTG-type calc-alkaline igneous suites (Bechiri-Benmerzoug 2009); (d) ultrahigh-temperature granulite metamorphism (e.g., Ouzegane et al. 2003); (e) gravity and magnetic anomalies related to spatial variations of lithosphere characteristics (Ayadi et al. 2000).

According to Black et al.'s (1994), Fig. 1) nomenclature, the Hoggar terranes, numbered from West to East, comprise the following: (a) in Western Hoggar, 1. Tassendjanet, 2. In-Ouzzal, and the Pharusian belt composed of 3. Tin Zaouatene, 4. In-Tedeini, and 5. Silet (formerly Iskel); (b) in the polycyclic Central Hoggar located in between North-South trending 4°50′E and 8°30′E shear zones, the LATEA metacraton (acronym for 6. Laouni, 7. Azrou N'Fad, 8. Tefedest, 9. Egere-Aleksod), 10. Serouenout, and 11. Assode-Issalane; (c) in Eastern Hoggar, 12. Aouzegueur, 13. Djanet, 14. Edembo; and (d) 15. Tassili sedimentary cover.

1. *The Tassendjanet terrane* is formed by alkaline to subalkaline granites and rhyolites of Paleoproterozoic age (Caby and Andreopoulos-Renaud 1983) affected by a high-pressure pan-African metamorphism under amphibolite facies (\Caby 2003), a carbonate cover with stromatolite-bearing horizons is assumed to have a Mesoproterozoic age (Caby and Monié 2003). A complex Neoproterozoic arc terrane (the Ougda complex, Dostal et al. 1996) rooted by gabbro-dioritic arc plutons that intruded in part the carbonate cover, which is unconformably overlain by ≥ 6000 m andesite flows and volcanic greywackes (Tassendjanet/Akofou complex) (Berger et al. 2014).
2. *The In Ouzzal terrane* consists in Archean crustal units, composed of orthogneissic domes and green stone belts, strongly remobilized during the Paleoproterozoic orogeny (2000 Ma, Peucat et al. 1996). Ouzegane et al. (2003) summarize this UHT metamorphic history as two granulitic stages of high temperature: a prograde evolution with peak conditions around 9–11 kbar and 950–1050 °C, leading to the appearance of exceptional parageneses with corundum-quartz, sapphirine-quartz and sapphirine-spinel-quartz in Al-Mg granulites, Al-Fe granulites and quartzites; followed by retrograde event characterized by a pressure drop to 5–7 kbar. This retrograde event is marked by intrusive carbonatite bodies and the occurrence of leptynite veins. The major effects of the Pan-African orogeny inside the In Ouzzal terrane comprise brittle faults and high-level subcircular intrusions, mostly granitic in composition, with sharp contacts with the country rocks. During the Pan-African orogeny, the In Ouzzal terrane preserved its Archean and Eburnean characteristics, rheological, geochemical and geochronological, which corresponds to a metacratonic behaviour (Haddoum et al., 2013).
3. *Tin Zaouatene* high-T–low-P amphibolite facies gneiss, graphitic micaschist, migmatite and anatectic granite, high-K calc-alkalic granitoids, and greenschist facies molasse.
4. *The In Tedeini terrane* is considered juvenile with oceanic affinities (Black et al. 1994) constituted by a Neoproterozoic greenschist-facies intruded by poorly known batholiths and plutons in which emplacement was strongly linked to movements along the major shear zones (Boissonnas 2008).
5. *The Silet* (ex Iskel) terrane is a narrow, c. 700 km-long, c. 60 km-wide, north-south trending strip stretching along the 4°25′ meridian within Hoggar. It is inserted between the In-Teidini Neoproterozoic juvenile terrane to the west (Black et al. 1994) and the LATEA metacratonic microcontinent to the east. It is occupied by two Neoproterozoic volcano-sedimentary series, namely the Pharusian I and the Pharusian II, which experienced contrasting tectonic episodes that are separated by the intra-Pharusian unconformity (Bertrand et al. 1966). Intercalated mafic–ultramafic cumulate bodies have been interpreted as representing remnants of ophiolitic units (Black et al. 1994, and references therein). An extensive TTG's plutonic ensembles are exposed

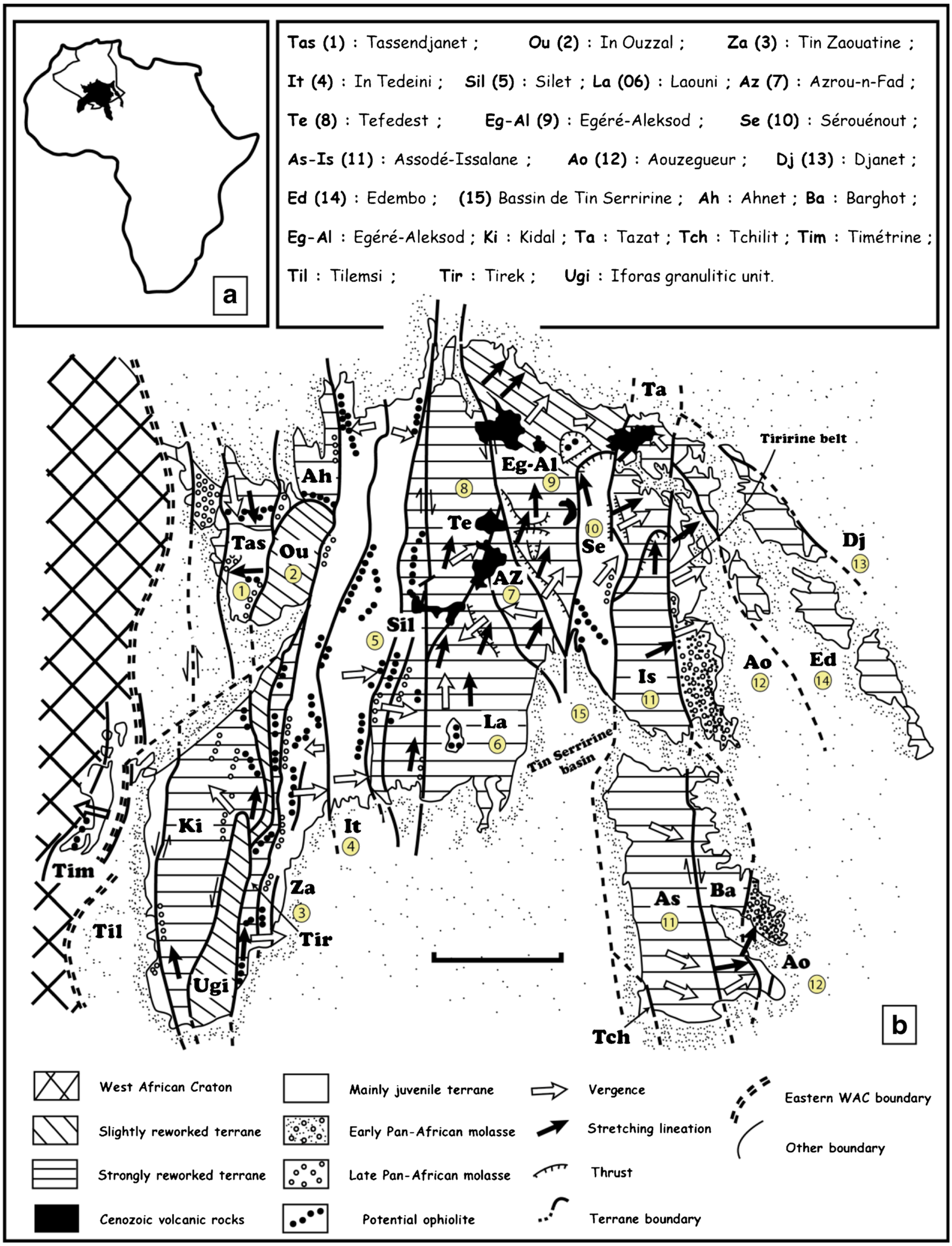

Fig. 1 **a** Schematic map of Africa showing location of Tuareg shield and Algeria. **b** Terrane map of Tuareg shield (Black et al. 1994, modified)

on central part of the terrane (Bechiri-Benmerzoug 2009) (Table 4). The igneous activity is older than the major Pan-African collisional stage, during which no igneous events occurred, in contrast with other parts of the Tuareg shield. Later on, Cambrian alkali-calcic granites of the "Taourirt" province were emplaced along Silet terrane boundaries (Azzouni-Sekkal et al. 2003). Most TTG's rocks are juvenile and show an oceanic arc affinity (Bechiri-Benmerzoug 2011).

LATEA metacraton: four terranes (Laouni, Azrou-n-Fad, Tefedest and Egere-Aleksod) are composed by Archean and Paleoproterozoic amphibolite to granulite-facies metamorphic and magmatic rocks (Peucat et al. 2003; Bendaoud et al. 2008 and references therein) that defined the metacraton LATEA (Liégeois et al. 2003, 2013). During Mesoproterozoic and Early and Middle Neoproterozoic, ocean terranes (such as the juvenile terrane of Silet—ex Iskel—and the Tin Begane eclogite-bearing nappes) were accreted along its margins during the Cryogenic and Ediacaran periods (Caby et al. 1982; Liégeois et al. 2003; Bechiri-Benmerzoug et al. 2009). Around 630 Ma begins the collision between the Tuareg/West African craton, during which LATEA craton has become a metacraton dissected into several terranes marked by emplacement of high-K calc-alkaline batholith derived partly from Paleoproterozoic/Archean crustal sources (Acef et al. 2003; Liégeois et al. 2003; Abdallah et al. 2007). The end of the process of metacratonization is marked by intrusion of shallow circular plutons, such as the Temaguessine pluton (cf. 580 Ma, Abdallah et al. 2007).

6. The *Laouni* terrane is composed of Archean-Paleoproterozoic granulite- to amphibolite-facies basement overthrust onto Pan-African lithologies, such as Tessalit ophiolitic remnant in the south and eclogite lenses and associated oceanic material in the Tin Begane area (Liégeois et al. 2003).
7. The *Azrou N'Fad* terrane is defined as a NW-SE trending slice of basement located in between Laouni and Egere-Aleksod terranes. The transgressive Early Paleozoic Tassili sandstones mark its southern tip. Archean-Paleoproterozoic granulitic gneisses and supracrustal formations were remobilized during the Pan-African orogeny and intruded by calc-alkaline batholiths (Ben El Khaznadji et al. 2017).
8. The *Tefedest* terrane is composed by basement orthogneiss with lenses of amphibolites and eclogites retromorphosed in the amphibolitic facies. The metasedimentary cover is formed by metapelites of ferruginous quartzites and marble (Briedj 1993). Pan-Africain magmatism is abundant in this area, with the calc–alkaline batholith of Azrou N'Fad, crosscut by the Temaguessine subcircular pluton dated at 582 ± 5 Ma (U–Pb/zircon; Abdallah et al. 2007).
9. The *Egéré* terrane: The Precambrian basement displays two metamorphic series. The Arechchoum orthogneissic migmatitic series and garnet amphibolite lenses, referred to as Egere series, are characterized by strongly flattened folds. Eclogites are associated with metapelites and marbles in metasediments (Arab et al. 2014), whereas they are missing in Arechchoum orthogneiss, which led the authors to interpret the contact between the two series as tectonic in nature (Doukhari et al. 2015).
10. The *Sérouènout* terrane (Fig. 1b) consists mainly of metasediments considered to have formed in an old oceanic domain involved in Neoproterozoic convergence and subsequent continental collision (e.g., Bertrand and Caby 1978; Caby 2003; Liégeois et al. 2003). However, ophiolitic markers of oceanic lithosphere are scarce in this region. Peridotitic and gabbroic rocks, exposed in the south of the terrane, have been considered remnants of oceanic lithosphere (e.g., Bertrand and Caby 1978; Caby 2003), but they do not yield the high-P metamorphism typical of subduction zones. The only high-P rocks reported so far in the Sérouènout Terrane have been observed in the Ti-N-Eggoleh area (Adjerid et al. 2015 and references therein).
11. The *Assodé–Issalane* terrane extends on 800 km from north to south (Fig. 1) and is characterized by high-temperature amphibolite facies metamorphism accompanied by regional K-rich leucogranite and by numerous high-K calc-alkaline batholiths and plutons dated between 620 and 570 Ma (Guérangé and Lasserre 1971; Bertrand et al. 1978; Liégeois et al. 1994). The metamorphic basement is a high-grade assemblage of banded and veined granitic to granodioritic gneisses and of a metasedimentary formation made up of fuschsite-bearing quartzites, calc-silicate gneisses and marbles. The whole was highly deformed under ductile conditions (Henry et al. 2009).
12. The *Aouzegueur* terrane, east of the Raghane shear zone, comprises a c. 730-Ma assemblage reminiscent of an oceanic environment (Caby and Andreopoulos-Renaud 1987) and a detrital sedimentary sequence (the Tiririne Group) separated from the former by an angular unconformity and intruded by a series of granitoid plutons and batholiths. The Tiririne Group becomes more metamorphic and more deformed northward: tight folds with N–S axial plane close to the 8°30 shear zone characterize the northern half of the area, while moderate folding affected the southern half. Greenschist-facies conditions are locally reached in the south, while they are more developed in the north (Henry et al. 2009).
13. The *Djanet* terrane is composed of detrital sedimentary series (Djanet Group), which was affected by greenschist-facies metamorphism. The Group is crosscut by magmatic intrusions between 571 and 558 Ma, related to the Late Ediacaran Murzukian orogenic episode, which has affected the Eastern Hoggar between 575 and 555 Ma (Fezaa et al. 2010).
14. The *Edembo* terrane is NW–SE elongated and bounded by shear zones adjacent to the Djanet terrane (Fig. 1b). It is characterized by amphibolite-facies metamorphism with abundant migmatites (e.g., Ouhot Complex, Table 5) and strong ductile deformation. Lithologies include biotite micaschists, metagreywackes with pebbles, phlogopite

marbles, hornblende metabasalts, and migmatitic gneisses (Fezaa et al. 2010).

15. The *Tin Serririne–Tin Mersoi* basin, southeast of the Hoggar shield in Algeria and Niger, is constituted by Paleozoic series overlying the Hoggar basement. Near In Guezzam, the lower part of the series is composed by slightly metamorphosed magmatic and sedimentary complexes of Cambrian age. Other Paleozoic sedimentary formations include Ordovician to Carboniferous series in Algeria and to Permian in Niger (Djellit et al. 2006).

The aim of this paper is to review all radiometric dates concerning the Hoggar and published from 1963 up to as of 2017 (Tables 1, 2, 3, 4, 5, 6, 7). The data will be discussed separately afterwards.

Historical foundations of Hoggar geology

The knowledge of the historical geology of Hoggar was acquired quite recently. Field works and map making started in the nineteenth century and developed since the early twentieth century (e.g., Gautier 1908, 1928). Major breakthroughs are owed to Conrad Kilian (1898–1950) and, later on, Maurice Lelubre (1916–2005).

Conrad Kilian established definitely the following points:

(a) Crystalline schists, reported previously as deformed Silurian formations, and granites are actually Precambrian in age. They are overlain unconformably by Tassili lower sandstones ("Grès inférieurs des Tassilis") that are, in turn, conformably overlain by Silurian fossiliferous shales and upper sandstones ("Grès supérieurs") (Killian 1924).

(b) The Precambrian stratigraphy comprises two members. The older, highly metamorphosed "Suggarian" is separated from the younger, weakly metamorphosed "Pharusian" by a major unconformity decorated with metamorphic conglomerates (Killian 1932).

(c) Another unconformity, marked again by conglomerates, was described by Karpoff (1946) in the Adrar des Iforas, the South- Western prolongation of Hoggar. It was recognized later on within the Pharusian. The Pharusian was then subdivided into an older "Relaidinian" and a younger "Nigritian" (Kilian 1947), two terms that never gained wide acceptance (Fig. 1).

In his Thesis Memoir Lelubre (1952), Maurice Lelubre applied successfully these subdivisions in a huge territory in Western and Central Hoggar. His interpretation of the "Pharusian" and the "Suggarian" as representing two successive orogenic cycles constituted a historical milestone in Hoggar geology.

The term "Pharusian" is still in usage. It matches Neoproterozoic formations that are currently subdivided into "Pharusian I" and "Pharusian II" (Bertrand et al. 1966), two terms replacing the former "Relaidinian" and "Nigritian", respectively. When isotopic ages became available, the "Suggarian" was shown to correspond to highly metamorphosed Archean and Paleoproterozoic formations, but also to some Neoproterozoic formations as well, so that the term became obsolete.

During the 50s of the last century, many field works were performed, either for academic theses, or for economic geology purposes, but no radiometric data were available. Then, geochronological laboratories developed dramatically worldwide and produced an increasing number of isotopic ages. As analytical apparatus and methods were considerably improved during the 80s of the last century, isotopic data will be presented in two parts: (1) data collected before 1980 and (2) data collected after 1980.

Analytical methods

Several analytical methods have been used in order to obtain meaningful ages in terms of geological events. Whether they succeeded, or not, is the subject of this paper. All methods are based on natural and artificial radioactivity and assume closed systems. Because dated formations in Hoggar either are Precambrian, or lack carbon as a major component, the ^{14}C method was not applied. Current methods apply either to mineral, or to whole-rock systems. They differ by the parent–daughter couples measured and by their temperatures of closure.

The Rb-Sr isotopic system

The Rb-Sr isotopic system was widely used in granitoids and gneisses, because they are generally rich in Rb and variously depleted in Sr. Single mineral (e.g., muscovite, biotite) or whole-rock dates should use an assumed value of initial $^{87}Sr/^{86}Sr$ (generally, 0.712). For minerals rich in Rb and poor in Sr (e.g., mica), that does not matter too much.

Results are not equally reliable and depend on the mineral analysed and the temperature, under which the system is closed, e.g., 500–300 °C for muscovite, 350–300 °C for biotite. Dates represent nothing more than cooling ages, which vary according to closure temperatures of minerals. Any thermal event raising temperature above closure temperatures will reset the isotopic clock.

Using mineral(s)–whole-rock isochrons has the advantage to give reasonable initial $^{87}Sr/^{86}Sr$ values. Whole-rock isochrons are even better, as isotopic closure is considered to take

Table 1 Isotopic ages published before 1980. Data arranged by terrane numbers

Aeon/Era	Area	Terrane	No. terrane	Location	Geological formation and/or rock	Isotopic systematics	Age (Ma)	Uncertainty	Authors' interpretation	References
Archean	Western Hoggar	In Ouzzal	2	Adrar Tanezrouft	Alkali granites	Rb-Sr WR isochron	2764	138	Igneous emplacement	Ferrara and Gravelle (1966)
							2711	135		
							2747	137		
				Alouki-Tin Tchik Tchik area	Charnockitic paragneiss	U-Th-Pb zircon	3300	20	Magmatic or metamorphic event	Lancelot et al. (1976)
							2900	0		
	Central Hoggar	Egéré—Aleksod	9	Gour Oumelalen	Red gneiss complex	Pb-Pb zircon	3476	60	Igneous emplacement	Latouche (1978)
						Rb-Sr WR isochron	3300	0	Igneous emplacement	Latouche and Vidal (1974)
							2400	0		
Paleproterozoic	Western Hoggar	Tassendjanet	1	Ouallen (sample 1192)	Migmatitic granite (Bio + Mus)	Rb-Sr muscovite	1795	50	Metamorphic event	Lay and Ledent (1963)
				Ouallen (sample 1191)	Migmatitic granite (Bio + Mus)	$^{207}Pb/^{206}Pb$ zircon	1885	80	Magmatic or metamorphic event	Lay et al. 1965)
				Ouallen (sample 1192)		K-Ar muscovite	1640	0		
		In Ouzzal	2	In Ouzzal	Biotite pegmatite	K-Ar biotite	1820	50	Igneous emplacement	Eberhardt et al. (1963)
						Rb-Sr biotite	1730	70	Igneous emplacement	
				Adrar Tanezrouft	Metamorphic rock	Rb-Sr biotite	1836	55	Metamorphic event	Ferrara and Gravelle (1966)
					Alkali granites		1788	54		
					Metamorphic rock		1769	53		
					Metamorphic rock	K-Ar biotite	1765	53	Metamorphic event	
					Alkali granites		1750	52	Igneous emplacement	
					Metamorphic rock		1690	52	Metamorphic event	
				In Ouzzal	Carbonatite	U-Pb-Th apatite	2090	0	Igneous emplacement	Allègre and Caby (1972)
					Granulite	Rb-Sr and K-Ar minerals	1860	0	Metamorphic event	
				Alouki-Tin Tchik Tchik area	Charnockitic paragneiss	U-Pb zircon	2170	30	Igneous emplacement	Lancelot et al. (1976)
						U-Th-Pb zircon	2040	30	Metamorphic event	
Paleproterozoic	Central Hoggar	Egéré—Aleksod	9	Aleksod area	Charnockite	Rb-Sr WR isochron	2000	0	Metamorphic event	Latouche and Vidal (1974)
				Gour Oumelalen	Hyperstene-bearing leucogranulites		1870	30		
					Marble	Rb-Sr phlogopite	1600	0	Metamorphic event	
Paleproterozoic	Central Hoggar	Egéré—Aleksod	9	Aleksod area	Tonalitic gneisses (O. Ouadenki)	Rb-Sr WR isochron	2220	60	Metamorphic event	Bertrand and Lassere (1976)
					Gniesses (Talat Mellet)		1940	50		

Table 1 (continued)

Aeon/Era	Area	Terrane	No. terrane	Location	Geological formation and/or rock	Isotopic systematics	Age (Ma)	Uncertainty	Authors' interpretation	References
		Tefedest	6	Arechchoum series	Paragneisses (O. Irnezzouf)		2110	40		
				Arechchoum series	Gneiss and mobilizates	Rb-Sr WR isochron	2240	70	Metamorphic event	Bertrand and Lasserre (1973)
				Arechchoum series	Migmatitic gneisses (paleosome)	Rb-Sr WR isochron	1972	200	Metamorphic event	Vialette and Vitel (1979)
Mesoproterozoic	Western Hoggar	Tassendjanet	1	Ouallen	Migmatitic granite (Bio + Mus)	$^{207}Pb/^{235}U$ zircon $^{206}Pb/^{238}U$ zircon	1395 1100	35 30	Metamorphic event	Lay et al. (1965)
	Central Hoggar	Egéré—Aleksod	9	Arechchoum series	Mafic dykes	K-Ar amphibole	1460 1435	40 39	Igneous emplacement	Bertrand et al. (1972)
				Tifinanine	Quartzite	Rb-Sr WR isochron Rb-Sr muscovite	1157 1210	114 110	Metamorphic event	Boissonnas et al. (1964)
				Aleksod area	Paragneisses (Agenou Guelta)	Rb-Sr WR isochron	1050	35	Metamorphic event	Bertrand and Lassere (1976)
		Tefedest	8	Arechchoum series	K-feldspar within gneiss	Rb-Sr K-feldspar isochron	1346	97	No geological significance	Bertrand and Lasserre (1973)
				Arechchoum series	Migmatitic gneisses (leucosome)	Rb-Sr WR isochron	1330	70	Metamorphic event	Vialette and Vitel (1979)
Neoproterozoïc	Central Hoggar	Laouni	6	In Abalessa	Porphyritic granite	K-Ar biotite	610	20	Metamorphic event	Eberhardt et al. (1963)
				Anfeg (3407) Anfeg (3410)	Biotite granite Granodiorite	Rb-Sr biotite	700 635	35 30	Igneous emplacement	Lay and Ledent (1963)
				Tin Begane	Biotite micaschist	Rb-Sr biotite	555	25	Metamorphic event	Lay and Ledent (1963)
				Anfeg (3407) Anfeg (3410)	Biotite granite Granodiorite	$^{207}Pb/^{206}Pb$ zircon $^{207}Pb/^{206}Pb$ zircon	635 630	30 30	Igneous emplacement	Lay et al. (1965)
				Anfeg (3407)	Biotite granite	$^{207}Pb/^{235}U$ zircon	600	15		
				Anfeg (3407)	Biotite granite	$^{206}Pb/^{238}U$ zircon	595	15		
				Tifferkit	Subcircular biotite granite	Rb-Sr WR isochron	546	6	Igneous emplacement	Vialette and Vitel (1979)
		Tefedest	8	In-Ecker (sample 127)	Muscovite schist	Rb-Sr muscovite	570	30	Igneous emplacement	Lay and Ledent (1963)
				Torsournine (sample 3405)	Biotite muscovite granite	$^{207}Pb/^{206}Pb$ zircon	665	30	Igneous emplacement	Lay et al. (1965)
				Torsournine (sample 3406)		$^{207}Pb/^{206}Pb$ zircon	655	30		
				Torsournine (sample 3406)		$^{207}Pb/^{235}U$ zircon	555	15		
					In Ozzaf granodiorite	Rb-Sr WR isochron	670	20		

Table 1 (continued)

Aeon/Era	Area	Terrane	No. terrane	Location	Geological formation and/or rock	Isotopic systematics	Age (Ma)	Uncertainty	Authors' interpretation	References
				Amsinassène group					Igneous emplacement	Vialette and Vitel (1979)
				Amsinassène group	In Teferkit biotite-muscovite granite	Rb-Sr WR isochron	545	9		
Neoproterozoïc	Central Hoggar	Egéré—Aleksod	9	Arechchoum series	Gneiss	Rb-Sr WR-biotite-K-feldspar isochron	540	23	Thermal event	Bertrand and Lasserre (1973)
				Gour Oumelalen	Zirmerzzouk (quartzite)	Rb-Sr muscovite	920	0	Thermal event	Latouche and Vidal (1974)
				Gour Oumelalen	Ounane (granodiorite)	Rb-Sr WR-biotite	565	0	Igneous emplacement	
				Aleksod series	Amphibolite	K-Ar hornblende	950	50	Metamorphic event	Bertrand and Lassere (1976)
				Aleksod area (Talat Mellet)	Mica-rich gneisses	Rb-Sr WR isochron	930	15		
				Série de l'Aleksod	Banded and blastomylonitic gneisses	Rb-Sr WR isochron	910	35	Metamorphic event	
				Aha'n'Souri	Granodiorite	Rb-Sr WR isochron	581	50	Igneous emplacement	
				Arechchoum	Gneiss	K-Ar amphibole	714	25	Igneous emplacement	Bertrand et al. (1972)
							658	18		
							624	17		
							580	16		
					Mafic dykes	K-Ar amphibole	647	18		
							617	17		
				Egere	Amphibolite-pyroxenite	K-Ar amphibole	974	25		
							933	26		
							926	26		
							914	25		
							720	20		
							697	19		
				Tallat Mellet	Amphibolite	K-Ar amphibole	706	20		
							649	18		
							622	17		
							616	18		
				Oued Aha'n'Souri	Granodiorite	K-Ar amphibole	595	17		
				Foum Haraou	Biotite-bearing granite	Rb-Sr biotite	570	16	Igneous emplacement	Boissonnas et al. (1964)
				Oued Tesjert (Arechchoum)	Migmatite	Rb-Sr biotite	576	23	Metamorphic event	

Table 1 (continued)

Aeon/Era	Area	Terrane	No. terrane	Location	Geological formation and/or rock	Isotopic systematics	Age (Ma)	Uncertainty	Authors' interpretation	References
				Tifoudjidjine	Migmatitic gneiss	Rb-Sr WR isochron	968	100	No geological significance	
						Rb-Sr muscovite	626	9	Metamorphic event	
Neoproterozoïc	Central Hoggar	Egéré—Aleksod	9	Temasint	Leptynite	Rb-Sr muscovite	751 693	10 35	Igneous emplacement	Guérangé et al. (1971)
				Azeguelalah	Granite margin	Rb-Sr biotite	547	25		
				Tazat	Orthogneiss	Rb-Sr muscovite	650	50		
						Rb-Sr biotite	650	30		
							614	31		
						Rb-Sr biotite-muscovite-W-R isochron	561	56		
					Quartzite	Rb-Sr muscovite	949	36		
						Ar-K biotite	578	15		
					Metarhyolite biotite	Rb-Sr biotite	658	33		
		Serouenout	10	Serouenout	Micaschist	Rb-Sr muscovite	960	95	Metamorphic event	Lay and Ledent (1963)
				Nazoubir (sample 523)	Biotite amphibole granite	$^{207}Pb/^{206}Pb$ zircon	650	30	Igneous emplacement	Lay et al. (1965)
				Nazoubir (sample 522)		$^{207}Pb/^{206}Pb$ zircon	625	30		
				Nazoubir (sample 522)		$^{207}Pb/^{235}U$ zircon	565	15		
				Nazoubir (sample 522)		$^{206}Pb/^{238}U$ zircon	545	15		
	Western Hoggar	Tassendjanet	1	Ouallen (sample 1192)	Migmatitic granite (Bio + Mus)	Rb-Sr biotite	745	35	Igneous emplacement	Lay and Ledent (1963)
		In Ouzzal	2	In Zize	Rhyolite	Rb-Sr WR isochron	550	30		
				In Hihaou	Granulite	Rb-Sr WR isochron	620	10	No geological significance	Allègre and Caby (1972)
		Tin Zaouatene	3	In Rabir (sample 2)	Microcline granite	Rb-Sr biotite	620	30	Igneous emplacement	Lay and Ledent (1963)
				Tin Touafa (sample 1808)	Biotite muscovite granite	$^{207}Pb/^{206}Pb$ zircon	590	40	Igneous emplacement	Lay et al. (1965)
				Tinnirt (sample 2048)	Microcline granite	$^{207}Pb/^{206}Pb$ zircon	610	30		
		In-Tedeini	4	Imezzarene	Granite margin	K-Ar biotite	640	20	Metamorphic event	Eberhardt et al. (1963)
				Iskel	Taourirt granite	Rb-Sr WR isochron	564	40	Igneous emplacement	Boissonnas et al. (1969a)
		Silet	5	Tioueiine			560	40		

Table 1 (continued)

Aeon/Era	Area	Terrane	No. terrane	Location	Geological formation and/or rock	Isotopic systematics	Age (Ma)	Uncertainty	Authors' interpretation	References
Neoproterozoïc	East Hoggar	Assode-Issalane	11	Honag shear zone	Adaf synkinematic monzogranite	U-Pb zircon	604	13	Igneous emplacement	Bertrand et al. (1978)
					Adaf late kinematic prophyritic monzogranite		585	14		
Neoproterozoïc	East Hoggar	Assode-Issalane	11	Honag	Biotite-bearing granite	Rb-Sr/biotite	561	17	Igneous emplacement	Guérangé et al. (1971)
						Rb-Sr WR-biotite-K-feldspar isochron	553	15		
Paleozoic	Western Hoggar	Tin Zaouatene	3	Tin Touafa (sample 1808)	Biotite muscovite granite	Rb-Sr biotite	525	15	Igneous emplacement	Lay and Ledent (1963)
				Tinnirt (sample 2048)	Microcline granite	Rb-Sr biotite	520	25		
				In Rabir (sample 1)	Biotite granite		510	15		
				Tin Touafa (sample 1808)	Biotite muscovite granite	Rb-Sr WR	510	100		
				Ti-N-Missaou	Muscovite quartzite		505	60		
				Tinnirt (sample 2048)	Microcline granite	$^{207}Pb/^{235}U$ zircon	440	15	Igneous emplacement	Lay et al. (1965)
				Tinnirt (sample 2048)	Microcline granite	$^{206}Pb/^{238}U$ zircon	410	15		
				Tin Touafa (sample 1808)	Biotite muscovite granite	$^{207}Pb/^{235}U$ zircon	390	20	Thermal event	
				Tin Touafa (sample 1808)	Biotite muscovite granite	$^{206}Pb/^{238}U$ zircon	355	15		
		In-Tedeini	4	Imezzarene	Granite margin	Rb-Sr biotite	535	20	Igneous emplacement	Eberhardt et al. (1963)
				Elbema (2023)	Biotite muscovite granite	Rb-Sr biotite	480	15	Igneous emplacement	Lay and Ledent (1963)
				Issedienne (5667)	Biotite-bearing granite	Rb-Sr biotite	470	15		
				Tesnou	Pegmatite lepidolite	Rb-Sr mineral ages	522	11	Igneous emplacement	Boissonnas et al. (1964)
	Central Hoggar	Laouni	6	In-Abeless	Porphyritic granite	Rb-Sr biotite	508	18	Igneous emplacement	Eberhardt et al. (1963)
				Ouan Rechla	Pegmatite	Rb-Sr zinnwaldite	510	15	Igneous emplacement	Lay and Ledent (1963)
						Rb-Sr microcline	500	15		
				Aheleheg	Biotite granite	Rb-Sr zinnwaldite	495	15		
				Ouan Rechla	Pegmatite		470	15		
				Anfeg (3410)	Granodiorite	$^{207}Pb/^{235}U$ zircon	525	15	Igneous emplacement	Lay et al. (1965)
						$^{206}Pb/^{238}U$ zircon	505	15		
				Taessa	Northern margin (granite)	Rb-Sr biotite	520	10	Igneous emplacement	Boissonnas et al. (1964)
				Torak	Centre (granite)	Rb-Sr biotite	480	29		

Table 1 (continued)

Aeon/Era	Area	Terrane	No. terrane	Location	Geological formation and/or rock	Isotopic systematics	Age (Ma)	Uncertainty	Authors' interpretation	References
				Gara Adjemamaye	Peralkaline granite	Rb-Sr WR-minerals	520	20	Igneous emplacement	Boissonnas et al. (1970)
				Taessa Granite	Gneiss	Rb-Sr biotite	520	10		
				In Tounine	Muscovite granite	Rb-Sr muscovite	497	19		
						Rb-Sr WR isochron	482	68		
				Torak Granite	Gneiss	Rb-Sr biotite	480	29		
Paleozoic	Central Hoggar	Tefedest	8	Torsournine (sample 3405)	Biotite amphibole granite	Rb-Sr muscovite Rb-Sr biotite	540 445	40 30	Igneous emplacement	Lay and Ledent (1963)
				Tan Afella Granite	Biotite muscovite monzogranite	Rb-Sr biotite Rb-Sr muscovite	532 532	7 8	Igneous emplacement	Boissonnas et al. (1964)
						Rb-Sr WR isochron	520	80		
				Oued Dehine granite	Biotite granite	Rb-Sr biotite	416	10	Igneous emplacement	Boissonnas et al. (1964)
				Tidikmar	Biotite granite	Rb-Sr biotite	417	8		
				Torsournine (sample 3406)	Biotite amphibole granite	$^{206}Pb/^{238}U$ zircon	530	15	Igneous emplacement	Lay et al. (1965)
				Dehine group	In Akoulmou calc-alkaline granite	Rb-Sr WR isochron	514	20	Igneous emplacement	Vialette and Vitel (1979)
		Egéré—Aleksod	9	Tifoudjidjine	Migmatitic gneiss	Rb-Sr biotite	506	16	Igneous emplacement	Boissonnas et al. (1964)
				Gour Oumelalen	Tissellilline (granite)	Rb-Sr WR-biotite	530	0	Igneous emplacement	Latouche and Vidal (1974)
				Aha'n'Souri	Granodiorite	Rb-Sr WR isochron	500	20	Igneous emplacement	Bertrand and Lassere (1976)
		Serouenout	10	Nazoubir (sample 443)	Biotite amphibole granite	Rb-Sr biotite	525	25	Igneous emplacement	Lay and Ledent (1963)
				Nazoubir (sample 444)			515	25		
				Nazoubir (sample 523)		$^{207}Pb/^{235}U$ zircon	540	15	Igneous emplacement	Lay et al. (1965)
				Nazoubir (sample 522)		Rb-Sr biotite	530	35		
				Nazoubir (sample 523)		$^{206}Pb/^{238}U$ zircon	515	15		
Cenozoic	Central Hoggar	Azrou-n-Fad—Tefedest boundary	7.8	Atakor	In Tahaïne trachytic ash	K–Ar WR	19.9 16.7	1.9 1.2	Igneous emplacement	Girod (1971)
					Akar Akar trachyte		14	0	Igneous emplacement	
					Tahat phonolite		12.4	2	Igneous emplacement	

Table 1 (continued)

Aeon/Era	Area	Terrane	No. terrane	Location	Geological formation and/or rock	Isotopic systematics	Age (Ma)	Uncertainty	Authors' interpretation	References
					Segaïka phonolite		6.7	0.2	Igneous emplacement	
					Hadriane trachyte		5.7	0.6	Igneous emplacement	
		Egéré—Aleksod	9	Amadghor Telleghteba	Trachyte		35	0	Igneous emplacement	Rossi et al. (1979)

Ma million years, *WR* whole-rock, *Bi* biotite, *FK* potassium feldspar

place as temperatures close to the granite solidus. However, this method should be used only in case of cogenetic samples, i.e., identical initial $^{87}Sr/^{86}Sr$ value, without any later disturbance. These required conditions are seldom completed, so that dates are only indicative and yield frequently large uncertainties (see Cahen et al. 1984).

The Sm-Nd isotopic system

This isotopic system presents the advantage that, contrary to Rb-Sr that may be mobile in hydrothermal environments, Sm and Nd are considered as immobile. Isotopic ages may be obtained via mineral(s), e.g., garnet, pyroxene, and/or whole-rock isochrons, following the same procedure as Rb-Sr. Closure temperatures for garnet are pretty high, i.e., 700–600 °C, and Sm-Nd datings involving garnet are fairly robust. If no isochrons can be obtained, due to isotopic heterogeneity, two model ages can be calculated, based on CHUR (CHondritic Uniform Reservoir) and DM (Depleted Mantle) evolution with time. Model ages are calculated in order to indicate when the source of the rock analysed was separated from CHUR, or DM. However, they are seldom meaningful in terms of geological history.

The isotopic systems containing Ar

Two methods are used, the conventional K-Ar method and the ^{39}Ar-^{40}Ar, in which ^{39}K is converted artificially in ^{39}Ar. The first method is used either on minerals, or on whole-rocks, especially in K-bearing mafic rocks that are too poor in Rb. The second method is suitable for K-bearing minerals, e.g., amphibole, biotite, and muscovite, and its advantage is that the two isotopic analyses are made on the same mass spectrometer. Recently, the method evolved to miniaturization, with laser ablation techniques. However, limitations due to closure temperatures are similar, or more severe than for Rb-Sr isotopic system, e.g., 550–450 °C for amphibole, 350–300 °C for muscovite, 320–250 °C for biotite, and 350–150 °C for feldspar.

The U-Pb isotopic systems

The dating method relies on two discrete decay chains, i.e., $^{238}U \rightarrow {}^{206}Pb$ and $^{235}U \rightarrow {}^{207}Pb$ that have different half-lives. Radioactive minerals that incorporate readily U and Th, but reject Pb, are suitable for U-Pb geochronology. Only Pb radiogenic isotopes can be detected in these minerals, with no Pb initial isotopic composition. Supplementary advantages of the dating method are high-closure temperatures, e.g., 900–750 °C for zircon, 700–600 °C for titanite, 500–400 °C for rutile, and 450–380 °C for apatite and monazite(Ce), and to provide two chronometers that can be compared in the same

Table 2 Archean isotopic ages published after 1980. Data arranged by terrane numbers

Aeon/Era	Area	Terrane	No. terrane	Location	Geological formation and/or rock	Isotope systematics	Age (Ma)	Uncertainty	Authors' interpretation	References
Archean	Western Hoggar	In Ouzzal	2	In Ouzzal	Charnockite (L101)	Sm-Nd WR model ages	3473	0	Igneous emplacement	Ben Othmane et al. (1984)
					Charnockite (M 408)		3123	0		
					Charnockite (M 408)	U-Pb zircon	3100	0		
					Charnockite (L101)	Rb-Sr WR model ages	3055	0		
					Charnockite (L101)	U-Pb zircon	2946	0		
				Ihaouhaoune	Quartzite (detrital zircon core)	U-Pb zircon	2900	200	Igneous emplacement	Hellal (1987)
				Tin Tchik Tchik	Tonalitic gneiss (Inz 91)	U-Pb zircon (SHRIMP and TIMS)	3270	11	Igneous emplacement	Peucat et al. (1996)
				Alouki-Khanfus-Ihouhouene	Detrital zircon (TH14-Inz105-Inh635)	U-Pb zircon (SIMS and TIMS)	3100	0	Igneous emplacement	Peucat et al. (1996)
				Afella	Monzogranitic gneisses (Inz81)	U-Pb zircon (SIMS)	2772	9		
				Tin Tchik Tchik	Tonalitic gneiss (Inz 87)	U-Pb zircon (SHRIMP)	2768	17		
				Afella, Tan Ataram, In Roccan	Granite gneiss (Inz73)	U-Pb zircon (SHRIMP and TIMS)	2731	6		
				Alouki-Khanfus-Ihouhouene	Detrital zircon (TH14-Inz105-Inh635)	U-Pb zircon (SIMS and TIMS)	2700	0		
				Afella, Tan Ataram, In Roccan	Granite gneiss (Inz73)	U-Pb zircon (SHRIMP and TIMS)	2650	10		
				Afella	Monzogranitic gneisses (Inz81)	U-Pb zircon (SIMS and TIMS)	2572	4		
				Tin Tchik Tchik	Granodioritic gneiss (Inz89)	U-Pb zircon (SHRIMP and TIMS)	2540	10		
					Tonalitic gneiss (Inz 91)		2506	15		
					Tonalitic gneiss (Inz 87)	U-Pb zircon (SHRIMP)	2540	11		
Archean	Central Hoggar	Egéré—Aleksod	9	Gour Oumelalen	Red gneiss complex (type1)	Sm-Nd WR	3100	100	Anatectic protolith	Peucat et al. (2003)
					Red gneiss complex (type 2)	Sm-Nd WR	2750	100	Igneous emplacement	
					Red gneiss complex (type 1-sample 677 + 659)	U-Pb zircon (TIMS and SIMS)	2716	18	Igneous emplacement	
					Red gneiss complex (type 1-sample 677)	U-Pb zircon (SIMS)	2696	21	Igneous emplacement	
					Red gneiss complex (type 1-sample 659)	U-Pb zircon (TIMS)	2647	18	Igneous emplacement	
					Red gneiss complex	^{207}Pb-^{206}Pb zircon (recalculated from Latouche 1978)	2568	120	Igneous emplacement	
Archean	East Hoggar	Djanet	13	Djanet Group	Conglomerate	U-Pb zircon (LA-ICP-MS)	3232	0	Detrital zircon deposited in sediments	Fezaa et al. (2010)
							2844	0		
							2800	0		
							2650	0		
		Edembo	14	Ouhot	Migmatite (protolith)	U-Pb zircon (SHRIMP)	2940	17	Anatectic protolith	

Table 3 Paleoproterozoic isotopic ages published after 1980. Data arranged by terrane numbers

Aeon/Era	Area	Terrane	No. terrane	Location	Geological formation and/or rock	Isotope systematics	Age (Ma)	Uncertainty	Authors' interpretation	References
Paleproterozoic	Western Hoggar	Tassendjanet	1	Adrar Tideridjaouine	Subalkaline metarhyolite	U-Pb zircon (TIMS)	1755	10	Igneous emplacement	Caby and Andreopoulos (1983)
		In Ouzzal	2	Ihaouhaoune	Quartzite (detrital zircon rim)	U-Pb zircon (TIMS)	2000	0	Metamorphic events	Hellal (1987)
				Ihouhaouene	Carbonatite (Inh641)	U-Pb zircon (TIMS)	1994 1994	22 17-	Igneous emplacement	Bernard-Griffiths et al. (1988)
				Ihouhaouene	Granulite	^{40}Ar-^{39}Ar biotite	1775	0	Igneous emplacement	Maluski et al. (1990)
				Tin Tchik Tchik	Tonalitic gneiss (Inz 87)	U-Pb zircon (SHRIMP)	2020	25	Metamorphic event	Peucat et al. (1996)
				Afella and Alouki	Meta-anorthosite (Inz12)	U-Pb zircon (SIMS and TIMS)	2002	7	Igneous emplacement	
				Khanfuss	Metasediment (Inz102)	Rb-Sr WR-garnet	2002	35	Metamorphic events	
				Tin Tchik Tchik	Granodioritic gneiss (Inz89)	U-Pb zircon (SIMS and TIMS)	2000	8		
				Alouki	Cordierite-bearing granitic gneiss (Inz9)	U-Pb zircon (TIMS)	2000	14	Igneous emplacement	
				Alouki-Khanfus-Ihouhouene	Detrital zircon (TH14-Inz105-Inh635)	U-Pb zircon (SIMS and TIMS)	2000	0	Metamorphic events	
				Afella	Cordierite granitic gneiss (Inz80)	U-Pb zircon (SHRIMP)	1983	15	Igneous emplacement	
				Alouki	Metasediment (Th 14)	Rb-Sr WR-garnet	1974	30	Metamorphic events	
				In Roccan area	Metasediment (Inz37)	Rb-Sr WR-garnet	1965	49		
				Khanfuss	Metasediment (Inz102)	Rb-Sr WR-garnet-rutile	1952	0		
				Khanfuss	Metasediment (Inz102)	Rb-Sr WR-silimanite-garnet-rutile isochron	1950	26		
				Khanfuss	Metasediment (Inz98)	Rb-Sr WR-biotite	1814	41		
				Alouki	Metasediment (Th 14)	Rb-Sr WR-biotite	1696	34		
Paleproterozoic	Central Hoggar	Laouni	6	Tidjenouine	Granulitic orthogneiss (TJ5)	U-Pb zircon (LA-ICP-MS)	2151 2062	8 39	Anatectic protolith Metamorphic event	Bendaoud et al. (2008)
		Egéré—Aleksod	9	Telohat	Migmatite (protolith)	U-Pb zircon upper intercept	2131	12	Anatectic or metamorphic event	Barbey et al. (1989)
				Gour Oumelalen	Supergroup (granulitic gneiss 673)	U-Pb zircon (SIMS) U-Pb zircon (TIMS)	2190 2183	5 1	Igneous emplacement	Peucat et al. (2003)
					Red gneiss complex (type 3)	Sm-Nd WR	1950	50	Igneous emplacement	
					Red gneiss complex (type 2-sample 2271)	U-Pb zircon (SIMS)	1903	3	Igneous emplacement	

Table 3 (continued)

Aeon/Era	Area	Terrane	No. terrane	Location	Geological formation and/or rock	Isotope systematics	Age (Ma)	Uncertainty	Authors' interpretation	References
					Red gneiss complex (type 2-sample 2267)	U-Pb zircon (TIMS)	1893	52	Igneous emplacement	
					Supergroup (Charnockite 734)	U-Pb zircon (TIMS)	2323	1	Igneous emplacement	
					Supergroup (Charnockite 731)		1958	3		
					Supergroup (Pegmatite 730)	U-Pb zircon (TIMS)	1904	3	Metamorphic events	
		Laouni	6	North Tin Amzi area	Iherane gneiss and migmatite	U-Pb zircon (TIMS)	2075	30	Metamorphic event	Bertrand et al. (1986a)
Paleoproterozoic	East Hoggar	Djanet	13	Djanet Group (detrital zircon)	Conglomerate	U-Pb zircon (LA-ICP-MS)	2438	0	Xenocrystic zircon deposited in sediments	Fezaa et al. (2010)
							2402	0		
							1908	0		
				Djanet Group (detrital zircon)	Sandstone		2014	0		
							1892	0		
		Edembo	14	Ouhot	Migmatite	U-Pb zircon(SHRIMP)	1831	16		

sample. Best cases are identical ages plotting on the concordia curve in the $^{206}Pb/^{238}U$–$^{207}Pb/^{235}U$ diagram.

Analytical techniques have developed throughout the last decades of the twentieth century. In the early days, poorly precise apparatus required large populations of crystals, hiding the intrinsic complexity of each grain, especially in the case of zircon. Zircon is very chemically inert and resistant to mechanical weathering, so that zones or even whole crystals can survive melting of parent rock with their original uranium-lead age intact. Thus, crystals with prolonged and complex histories may contain zones of strikingly different ages (usually, with the oldest and youngest zones forming the core and rim, respectively, of the crystal).

Until the 90s of the last century, data interpretations were based on analytical results aligned along a straight line, named discordia, which crosscuts the concordia curve at upper and lower intercepts. Due to improvement of analytical techniques, the required masses of crystal populations became smaller and smaller, from milligrammes down to microgrammes. Currently, instead of populations, single crystals are selected on the basis of various criteria, such as typology and zonation examined by SEM imagery, to unravel their complex evolution from concordant data. Carefully selected single grains are still analysed via the highly precise thermal ionization mass spectrometry (TIMS). In situ micro-beam analyses are routinely performed via secondary ion microprobe spectrometry (SIMS) or laser ablation multi-collector inductively coupled plasma mass spectrometry (LA-MC-ICPMS).

Age precisions

According to techniques used, analytical errors on isotopic ratios are variable, ranging from 1 to 2% for old data down to less than 0.2% for recent ones. In published papers, age regressions were made using various softwares. Now, the most popular software package is ISOPLOT. Though the first purpose was to create a uranium-decay dating program (Ludwig 1991), the last updates, ISOPLOT 3.75 and ISOPLOT 4.15 (Ludwig 2012), can calculate and plot isochrons and concordia intercepts for a wide variety of isotopic systems.

Isotopic data published before 1980

To our knowledge, the very first published radiometric datings were made in 1960 using K-Ar method. They were followed in 1963 by two communications presented at the Academy of Sciences of Paris. The first was devoted to biotite ages via K-Ar and Rb-Sr methods (Eberhardt et al. 1963). The dated terranes were In Ouzzal (biotite pegmatite), Laouni (In Abalessa porphyritic granite) and In-Tedeini (Imezzarene

Table 4 Neoproterozoic isotopic ages published after 1980. Data arranged by terrane numbers

Aeon/Era	Area	Terrane	No. terrane	Location	Geological formation and/or rocks	Isotope systematics	Age (Ma)	Uncertainty	Authors' interpretation	References
Neoproterozoïc	Western Hoggar	Tassendjanet	1	Ougda volcanic arc	Mafic amphibolite (M775)	^{40}Ar-^{39}Ar amphibole	718.6	7.2	Metamorphic event	Caby and Monié (2003)
				Tideridjaouijne HP belt	Granulite	^{40}Ar-^{39}Ar phengite	611.1 588.2	5.1 4.9	Metamorphic event	
				In Tassak	Pelitic metatexite (C106) Amphibolite	^{40}Ar-^{39}Ar biotite ^{40}Ar-^{39}Ar amphibole	585.9 577.3	5.5 6.1	Metamorphic event	
				Tidéridjaouine	Eclogite (TINZ 3)	U-Pb zircon (LA-ICP-MS)	623	2	Metamorphic event	Berger et al. (2014)
				Tin Zebane (Dyke swarm)	Gabbros and granites	Rb-Sr WR isochron	592.2	5.8	Igneous emplacement	Hadj Kaddour et al. (1998)
		In Ouzzal	2	Ihaouhaouene	Carbonatite	Apatite fission tracks	628	0	Thermal event	Carpena et al. (1988)
				North Tihimatine	Sub-circular granitic pluton	U-Pb zircon (SHRIMP)	601	4	Igneous emplacement	Fezaa et al. (2011)
						U-Pb zircon (LA-ICP-MS)	600	5		
		In-Tedeini	4	Iskel	Taourirt granite	Rb-Sr WR isochron (recalculated from Boissonnas et al. (1969)	592	20	Igneous emplacement	Cahen et al. (1984)
				Imezzarène	Granite	U-Pb zircon	583	7	Igneous emplacement	Bertrand et al. (1986a, 1986b)
		Silet	5	Tin Dahar Tin Dahar	Tin-Tekadiouit tonalite Taklet granite	U-Pb zircon	868 839	8 4	Igneous emplacement	Caby et al. (1982)
				Tin Dahar	Irrelouchem volcanic series (basalt, rhyodacite and ignimbrites)	Rb-Sr WR isochron	680	36	Igneous emplacement	Dupont (1987)
				Tamteq Ahambatou	Tonalite (S37) Granodiorite (ID29)	U-Pb zircon (SHRIMP)	742 651	5 6	Igneous emplacement	Bechiri-Benmerzo-ug (2009)
				Silet	Inner monzogranite (S69)		649	5		
					Outer monzogranite (S72)		648	3		
				Anou-Eheli	Granodiorite (EH16)		638	5		
		Silet—Laouni boundary	5.6	Aouilene	Gneissic granite	U-Pb zircon (TIMS)	629	5	Igneous emplacement	Bertrand et al. (1986a, 1986b)
						U-Pb titanite (TIMS)	614	6		
Neoproterozoïc	Central Hoggar	Laouni	6	North Tin Amzi area	Anfeg (granodiorite and granite)	U-Pb zircon (TIMS)	615	5	Igneous emplacement	Bertrand et al. (1986a, 1986b)

Table 4 (continued)

Aeon/Era	Area	Terrane	No. terrane	Location	Geological formation and/or rocks	Isotope systematics	Age (Ma)	Uncertainty	Authors' interpretation	References
					Tin Amzi (granite)	U-Pb zircon (TIMS)	612	50	Igneous emplacement	
						U-Pb zircon (TIMS)	612	20-		
				Abalessa-Tinef	Orthogneiss	U-Pb zircon (TIMS)	604	10	Igneous emplacement	
						U-Pb zircon (TIMS)	604	6-		
				In Amguel area	Aou Zebaouene (granite)	U-Pb zircon (TIMS)	592	6	Igneous emplacement	
				Tifferkit	Subcircular biotite granite	^{40}Ar-^{39}Ar biotite	576	1.7	Igneous emplacement	Cheilletz et al. (1992)
				Tin Begane	Amphibole-bearing eclogite	Sm-Nd WR	685	60	Metamorphic events	Boughrara (1999)
				North Tin Amzi area	Anfeg (granodiorite and granite)	U-Pb zircon (recalculated after Bertrand et al. 1986)	608	7	Igneous emplacement	Acef et al. (2003)
				Tin Begane	Amphibolite Garnet amphibolite (675-TB) Eclogite (680-2b)	Sm-Nd WR-minerals	686 685 683	6 20 60	Metamorphic events	Liégeois et al. (2003)
				Tidjenouine	Granulitic orthogneiss (TJ5)	U-Pb zircon (LA-ICP-MS)	614	11	Metamorphic event	Bendaoud et al. (2008)
				In-Tounine	Alkali-calcic granite	U-Pb zircon (LA-ICP-MS)	552	3	Igneous emplacement	Abdallah et al. (2011)
				North Tin Amzi area	North Amsel (TTG) South Amsel (granite)	U-Pb zircon (LA-ICP-MS)	630 599	5 3	Igneous emplacement	Talmat-Bouzeguela et al. (2011)
		Egéré—Aleksod	9	Telohat	Migmatite (anatexis)	U-Pb zircon lower intercept	609	17	Metamorphic events	Barbey et al. (1989)
				Gour Oumelalen	Ounane pluton (granodiorite)	Rb-Sr WR isochron	624	15	Igneous emplacement	Liégeois et al. (2003)
					Tisselliline (granite)		555	15		
					Timegassine (Fe-cordierite orbicular granite)	U-Pb zircon (SHRIMP)	582	5	Igneous emplacement	Abdallah et al. (2007)
					Ounane pluton (granodiorite)	U-Pb zircon (SHRIMP)	629	6	Igneous emplacement	Abdallah (2008)
					Tihoudaïne		580	6		
					Tisselliline (granite)		572	6		
Neoproterozoïc			11	Honag shear zone	Adaf pluton (granite)		593	17	Igneous emplacement	Henry et al. (2009)

Table 4 (continued)

Aeon/Era	Area	Terrane	No. terrane	Location	Geological formation and/or rocks	Isotope systematics	Age (Ma)	Uncertainty	Authors' interpretation	References
	East Hoggar	Assodé—Issalane				U-Pb zircon (recalculated from Bertrand et al. (1978))				
		Aouzegueur	12	Arokam	Granodiorite	U-Pb zircon (TIMS)	729	8	Igneous emplacement	Caby and Andreopoulos-Renaud (1987)
				Raghane shear zone (Erg Kilian)	Arigher batholith (granite)	Rb-Sr WR isochron	556	20	Igneous emplacement	Zeghouane (2006)
					Arigher batholith (granite)	U-Pb zircon (LA-ICP-MS)	554	5	Igneous emplacement	Henry et al. (2009)
				Raghane shear zone	Oued Touffok pluton (granite)		793	4		
					Ohergehem granodiorite		594	4		
				Djanet-Tafassasset	Arif batholith (granite)	U-Pb zircon	750	5	Igneous emplacement	Abbassene and Oubadi (2010)
		Djanet	13	Djanet Group (detrital zircon)	Conglomerate	U-Pb zircon (LA-ICP-MS)	947	0	Xenocrystic zircon deposited in sediments	Fezaa et al. (2010)
							735	0		
							673	0		
							638	0		
							605	4		
							602	0		
							597	10		
				Djanet Group (detrital zircon)	Sandstone	U-Pb zircon (LA-ICP-MS)	712	0	Xenocrystic zircon deposited in sediments	
							648	0		
							595	0		
							591	10		
							589	11		
				Djanet batholith	Porphyritic granite	U-Pb zircon (SHRIMP)	571	16	Igneous emplacement	
				Tin-Bejane subcircular pluton	Syenogranite	U-Pb zircon (SHRIMP)	568	5		
				Tin-Amali dyke swarm	Granodiorite to monzogranite	U-Pb zircon (SHRIMP)	558	6		
		Edembo	14	Ouhot	Migmatitic gneiss	U-Pb zircon (SHRIMP)	675	15	Xenocrystic zircon deposition in sediments	
							596	10		
					Leucosome	U-Pb zircon (SHRIMP)	568	4	Metamorphic events	

Table 5 Paleozoic isotopic ages and low-temperature thermochronology published after 1980. Data arranged by terrane numbers

Aeon/Era	Area	Terrane	No. terrane	Location	Geological formation and/or rock	Isotope systematics	Age (Ma)	Uncertainty	Authors' interpretation	References
Paleozoic	Western Hoggar	In Ouzzal	2	Ihaouhaouene	Carbonatite	Apatite fission tracks	500	0	Thermal event	Carpena et al. (1988)
		In-Tedeini	4	Aït-Oklan Tesnou	Taourirt granite	Rb-Sr WR isochron	511 506	39 16	Igneous emplacement	Azzouni-Sekkal et al. (2003)
		Silet	5	Tioueine	Taourirt syenite	U-Pb zircon (SHRIMP)	523	1	Igneous emplacement	Paquette et al. (1998)
				Teg-Orak	Taourirt granite	Rb-Sr WR isochron	519	18	Igneous emplacement	Azzouni-Sekkal et al. (2003)
Paleozoic	Central Hoggar	Laouni	6	North Tin Amzi area	Iherane gneiss and migmatites	U-Pb zircon (lower intercept)	530	70	Metamorphic events	Bertrand et al. (1986a, 1986b)
				Debnat	Leucogranite	^{40}Ar-^{39}Ar biotite	538.7	2.4	Igneous emplacement	Cheilletz et al. (1992)
				In-Tounine	Biotite granite		534. 5	2.5	Igneous emplacement	
				Tin-Amzi El Karoussa	Leucogranite		536.1	2.2	Igneous emplacement	
				Hanana	Leucogranite		526.4	2.8	Igneous emplacement	
				Aheledj	Subcircular biotite granite		525.5	2.2	Igneous emplacement	
				In-Tounine	Biotite granite	Rb-Sr WR isochron	521	17	Igneous emplacement	
				In Tounine	Biotite granite	Rb-Sr WR isochron	502	42	Igneous emplacement	Azzouni-Sekkal et al. (2003)
				Baouinet Nord	Taourirt granite	Rb-Sr WR isochron	524	43	Igneous emplacement	
				Tin-Begane	Garnet gneiss (648-2) Garnet amphibolite (648-3) Greenschist facies Garnet amphibolite (661-1)	Sm-Nd WR-minerals	531 528 522 506	38 66 27 48	Metamorphic event	Liégeois et al. (2003)
		Azrou N'Fad	7	Gara Adjamamaye	Peralkaline granite	Rb-Sr WR isochron	526	22	Igneous emplacement	Kahoui et al. (2011)
Paleozoic	East Hoggar	Tin Seririne Basin	15	Tin Seririne	Dolerite	K-Ar WR	347.6	16.2	Igneous emplacement	Djellit et al. (2006)
		Tassilis		Arrikine	Gabbro	K-Ar WR	325.6	7.7	Igneous emplacement	Derder et al. (2016)

Table 6 Mesozoic low-temperature thermochronology published after 1980. Data arranged by terrane numbers

Aeon/Era	Area	Terrane	No. terrane	Location	Geological formation and/or rock	Isotope systematics	Age (Ma)	Uncertainty	Authors' interpretation	References
Mesosoic	Western Hoggar	In Ouzzal	2	Ihaouhaouene	Carbonatite	Apatite fission tracks	263	0	Thermal event	Carpena et al. (1988)
							247	0		
		Tin Zaouatene	3	Mouydir	Granodiorite (TOD128)	Apatite fission tracks	118	4	Thermal event	Rougier et al. (2012)
						U-Th/He apatite	92.5	7.4	Thermal event	
		In-Tedeini	4	Tesnou	Granite (TZA204)	Apatite fission tracks	89	8	Thermal event	
						U-Th/He apatite	70.3	4.9		
		Silet	5	Silet	Granodiorite (AIG2)	Apatite fission tracks	166	9	Thermal event	
					Granodiorite (AIG3)		166	10		
					Granodiorite (AIG1)		99	6		
				Tidjelamine	Granite (TZA28)	U-Th/He apatite	94.6	8.1	Thermal event	
					Granite (TZA28)	Apatite fission tracks	71	6	Thermal event	
Mesosoic	Central Hoggar	Laouni	6	In Tounine	Granite (IT22)	U-Th/He apatite	111	7.8	Thermal event	Rougier et al. (2012)
						Apatite fission tracks	96	11		
					Granite (IT05)	Apatite fission tracks	75	8		
		Egéré—Aleksod	9	Tisselliline	Granite (TOD30)	Apatite fission tracks	285	29		
				Ounane	Granodiorite (TOD27)	Apatite fission tracks	179	20		
				Tisselliline	Granite (TOD17)	Apatite fission tracks	111	10		
					Granite (TOD30)	U-Th/He apatite	82	19.3		
Mesosoic	East Hoggar	Assodé—Issalane	11	Tin Ghoras	Granite (ARO113)	Apatite fission tracks	114	10	Thermal event	Rougier et al. (2012)

margin granite), whereas the second dealt with K-Ar and Rb-Sr methods on phyllosilicates (biotite, muscovite, zinnwaldite) and whole-rocks, with preliminary data using U-Pb method on zircon (Lay and Ledent 1963). The dated terranes were Laouni (Anfeg batholith and Tin Begane biotite micaschist), Tassendjanet (Ouallen migmatitic granite), Tefedest (In-Ecker muscovite schist), Serouenout (micaschists) and Tin Zaouatene (In Rabir granite, Tin Touafa biotite muscovite granite, Tinnirt microcline granite and Ti-N-Missaou muscovite quartzite).

During the two decades 1960–1980, datings began to cover randomly the different Precambrian formations, with the aim to unravel the major events having built the shield (Fig. 2). Yet, geochronological studies were more focussed to the western terranes, owing to the discovery of Archean In Ouzzal high-grade granulitic formations. The available analytical apparatus was less improved than currently, and the quality of data was severely limited as in the following: (a) Rb-Sr, K-Ar and U-Pb results were largely discordant with ^{207}Pb-^{206}Pb > U-Pb > K-Ar ≥ Rb-Sr ages, (b) single mineral analyses precluded the use of isochrones or discordia curves, and (c) ages obtained on crystal populations were inherently flawed by isotopic heterogeneity.

In the early 1980s, a comprehensive framework for the Hoggar structure is identified mainly using the radiometric data (19 publications, 162 radiometric data; Table 1) and nine techniques: 1/− Rb-Sr minerals (56 analysis); 2/− Rb-Sr whole-rock isochron (30 analysis; Table 1); 3/− K-Ar minerals (amphibole, biotite and muscovite; 30 analysis); 4/− U-Pb zircon (28 analysis); 5/− K-Ar whole-rock (07 analysis); 6/− Rb-Sr whole-rock-minerals (06 analysis); 7/− U-Th-Pb zircon (02 analysis); 8/− Pb-Pb zircon (01 analysis); and 9/− U-Pb-Th apatite (01 analysis) (Table 1, Fig. 2).

Thus, the features evidenced by the data were approximate only. The major results, as of 1980, were as follows:

(1) The so-called Suggarian formations yielded an unexpected large age range from Archean to Neoproterozoic, thus questioning its reliability as a geological group. On the contrary, the Pharusian formations displayed a more restricted range of Neoproterozoic dates.
(2) Several orogenic episodes were substantiated: Archean events in cratonic fragments, Paleoproterozoic Eburnean orogeny, and Neoproterozoic Pan-African orogeny.
(3) Early Paleozoic dates would correspond to resetting by hydrothermal episodes related to strike-slip shear zones, before Tassili sandstone deposition in the Late Cambrian.
(4) Scarce Mesoproterozoic dates were interpreted as suggesting the possible role played by the Kibaran event defined in central-southern Africa (Table 1, Fig. 2).

Table 7 Cenozoic isotopic ages and low-temperature thermochronology published after 1980. Data arranged by terrane numbers

Aeon/Era	Area	Terrane	No. terrane	Location	Geological formation and/or rock	Isotope systematics	Age (Ma)	Uncertainty	Authors' interpretation	References
Cenozoic	Western Hoggar	Tin Zaouatene	3	Mouydir	Granodiorite (TOD128)	U-Th/He apatite	49	9.2	Thermal event	Rougier et al. (2012)
		In-Tedeini	4	Tesnou	Granite (TZA204)		10.1	0.7		
		Silet	5	Silet	Granodiorite (AlG3)		60.4	4.2		
					Granodiorite (AlG2)		56.3	4.5		
					Granodiorite (AlG3)		33.9	2.4		
					Granodiorite (AlG2)		30.5	2.4		
				Tidjelamine	Granite (TZA28)		20.6	3.8		
		Silet—Laouni boundary	5.6	Tahalgha	Trachyte	K–Ar WR	3.4	0.1	Igneous emplacement	Aït-Hamou and Dautria (1994)
					Alkali basalt		3.3	0.1		
					Rhyolite		3.1	0.07		
					Hawaiite		2.9	0.1		
					Alkali basalt		2.6	0.2		
					Basanite		2.5	0.08		
					Hawaiite		2.43	0.06		
Cenozoic	Central Hoggar	Laouni	6	In Tounine	Granite (IT05)	U-Th/He apatite	60.4	4.2	Thermal event	Rougier et al. (2012)
					Granite (IT05)		41.4	4.6		
					Granite (IT22)		33.4	2.7		
		Azrou-n-Fad	7	Atakor	Segaïka basanite	K–Ar WR	1.56	0.14	Igneous emplacement	
					Ilamane phonolite		6.6	0.3		
					Sesker Akr mugearite		5.3	0.2		
					Teguit basalt		4.2	0.2		
					Timesdelsine basalt		1.95	0.2		
				Téhéntawak (Manzaz)	Basanite	K-Ar WR-mesostasis	1.51	0.58	Igneous emplacement	Benmessaoud (2014)
				Azrou	Trachyte—phonolite	Rb-Sr WR isochron	23.1	1.6	Igneous emplacement	Ben El Khaznadji et al. (2017)
		Egéré—Aleksod	9	Amadghor/Pic Iharen	Trachyte	K–Ar WR	21.4	0	Igneous emplacement	Aït-Hamou and Dautria (1994)
					Basanite	K–Ar WR	8.2	0	Igneous emplacement	Aït-Hamou and Dautria (1994)
				Achkal ring complex	Outer gabbro	K-Ar WR	29	0.6	Igneous emplacement	Maza et al. (1995)
					Inner rhyolite		24	0.5		
					Basaltic dyke	K-Ar WR	25.8	0		
				Oua-n-Aressou ring complex	Outer gabbro	^{40}Ar-^{39}Ar biotite	24	0.5	Igneous emplacement	Maza et al. (1998)
					Inner monzonite		23.6	0.5		
				Achkal ring complex	Monzodioritic dyke	K-Ar WR	22	0	Igneous emplacement	
					Nephelinitic dyke		8	0		
					Syenitic dyke	K–Ar WR	34.8	0		
				Taharaq	Transitional trachybasalt	K–Ar WR	44	0.8	Igneous emplacement	Aït-Hamou et al. (2000)
						^{40}Ar-^{39}Ar WR	34.5	3.5		
						K–Ar WR	28.5	0.5		
						K–Ar WR	27.9	0.6		
						K–Ar WR	24.4	0.5		
					Transitional basalt lava flow	K–Ar WR	33.6	0.7	Igneous emplacement	
						^{40}Ar-^{39}Ar WR	33.6	5.7		
						K–Ar WR	33.4	0.8		

Table 7 (continued)

Aeon/Era	Area	Terrane	No. terrane	Location	Geological formation and/or rock	Isotope systematics	Age (Ma)	Uncertainty	Authors' interpretation	References
						^{40}Ar-^{39}Ar WR	32.8	2.6		
					Alkali basalt	K–Ar WR	28.9	0	Igneous emplacement	
						K–Ar WR	23.6	0.7		
					Trachyandesite	K–Ar WR	21.8	0.4	Igneous emplacement	
					Phonolite	K–Ar WR	20.7	1	Igneous emplacement	
				In-Roundoum	Trachyte	K–Ar WR	28	0	Igneous emplacement	
					Basaltic dyke	K–Ar WR	25.8	0		
					Monzonitic dyke	K–Ar WR	22.1	0		
				Ounane	Granodiorite (TOD27)	U-Th/He apatite	43.6	5.8	Thermal event	Rougier et al. (2012)
							4.6	0.8		
				Tisselliline	Granite (TOD17)	U-Th/He apatite	59.3	12.9		
							11.8	3.8		
					Granite (TOD30)	U-Th/He apatite	13.5	3.4		
		Serouenout	10	Oued Tafassasset	Basanite	^{40}Ar-^{39}Ar biotite	16.8	0.6	Igneous emplacement	Aït-Hamou and Dautria (1994)
				Gara Tiklatine	Basanite	K–Ar WR	16.1	0.4		
							13.6	0.5		
				Serouenout	Phonolite	^{40}Ar-^{39}Ar biotite	15.7	0.3	Igneous emplacement	Maza et al. (1998)
							13.2	0.3		
							14.2	0.3		
							11.63	0.24		
					Trachyte		13.3	0.3		
							12.9	0.3		
					Nephelinite		13.6	0.5		
							6	0.2		
							4.7	0.3		
Cenozoic	East Hoggar	Assodé—Issalane	11	Tin Ghoras	Granite (ARO113)	U-Th/He apatite	20.4	1.5	Thermal event	Rougier et al. (2012)
							12.9	2.6	Thermal event	
		Edembo	14	In Ezzane district	Basanite	K-Ar WR-mesostasis	2.86	0.07	Igneous emplacement	Yahiaoui et al. (2014)

(5) K-Ar datings of Atakor felsic volcanic rocks evidence Neogene episodes.

Isotopic ages published after 1980

Together with remarkable improvements of the analytical apparatus, sampling strategy changed, with datings focussed on restricted areas carefully selected with specific purposes, mostly for doctoral theses. All field studies (Fig. 3) are currently accompanied by geochronological data. Though the shield is still unevenly covered, more precise analytical results allowed more accurate deciphering of the geological history. In addition, recent attention was paid to the detrital zircon component of (meta)sedimentary formations, which explains in part the flood of data collected since the beginning of the twenty-first century.

Since 1980, over 243 radiometric data were published (47 publications), the most used technique in the Hoggar and probably in the world is U-Pb zircon (102 analysis, LA-ICP-MS, SHRIMP, TIMS and SIMS). Followed by K-Ar whole-rock (35 analysis), U-Th-Pb apatite (22 analysis), Ar-Ar minerals (21 analysis), fission track apatite (16 analysis), Rb-Sr whole-rock (15 analysis), Sm-Nd whole-rock-minerals (13 analysis), Ar-Ar whole-rock (11 analysis), Rb-Sr whole-rock-minerals (07 analysis), and U-Pb titanite (1) (Fig. 3, Tables 2, 3, 4, 5, 6). Increasingly precise ages due to improved measuring devices contributed to understand better the geodynamic evolution of the Hoggar.

All radiometric data conducted after 1980 by terranes are represented in Fig. 4. Three distinct periods are emphasized: (a) Archean-Paleoproterozoic (Tables 2 and 3), (b) Neoproterozoic-Early Paleozoic (Tables 4 and 5), and (c) Cenozoic (Table 7). The absence of Mesoproterozoic and Mesozoic (Table 6) is a major feature in the geodynamic evolution of the Hoggar shield.

Archean igneous episodes (Fig. 5, Table 2) were found exclusively in the In-Ouzzal, with e.g., 3473–2946 Ma charnockite (Ben Othmane et al., 1984; Sm-Nd, Rb-Sr WR model ages, U-Pb zircon), 3270 ± 11 to 2506 ± 15 Ma tonalitic gneisses (U-Pb zircon/SHRIMP and TIMS), 2772 ± 9 to 2572 ± 4 monzogranitic gneisses (U-Pb zircon/SIMS and TIMS) and 2731 ± 6 to 2650 ± 10 Ma granite gneiss (Peucat et al. 1996), and in the Egere-Aleksod terranes, with 2750 ± 100 to 2568 ± 120 Ma red gneiss complex (Sm-Nd WR and U-Pb/zircon TIMS and SIMS; Table 2) (Peucat et al. 2003) (Fig. 3a). For a more complete review, see Drareni et al. (2007).

Detrital zircon crystals found in quartzites (Ihaouhaoune, In-Ouzzal) yield cores at 2900 ± 100 Ma and rims at 2000 Ma (Hellal 1987; U-Pb zircon). In the Djanet terrane (Eastern Hoggar), xenocrystic zircon deposited in conglomerate yields also Archean ages (U-Pb zircon/LA-ICP-MS, 3232–2650 Ma, Fezaa et al. 2010). In the Edembo terrane, protolith of the Ouhot migmatite yields 2940 ± 17 Ma (U-Pb zircon (SHRIMP, Fezaa et al. 2010). The sources of Archean zircon crystals are likely the In Ouzzal and Egere-Aleksod terranes.

The Paleoproterozoic episodes identified by the authors before the 1980s (Fig. 2, Table 1) were confirmed by coeval magmatic and metamorphic events in the In-Ouzzal (around 2000 to 1700 Ma, Bernard-Griffiths et al. 1988; Maluski et al. 1990; Peucat et al. 1996) (Table 3) and the Egere-Aleksod terranes (around 2200–1900 Ma, Peucat et al. 2003) (Fig. 6). In the Tassendjanet terrane, a Paleoproterozoic igneous episode occurred at 1755 ± 10 Ma, whereas, in the Laouni

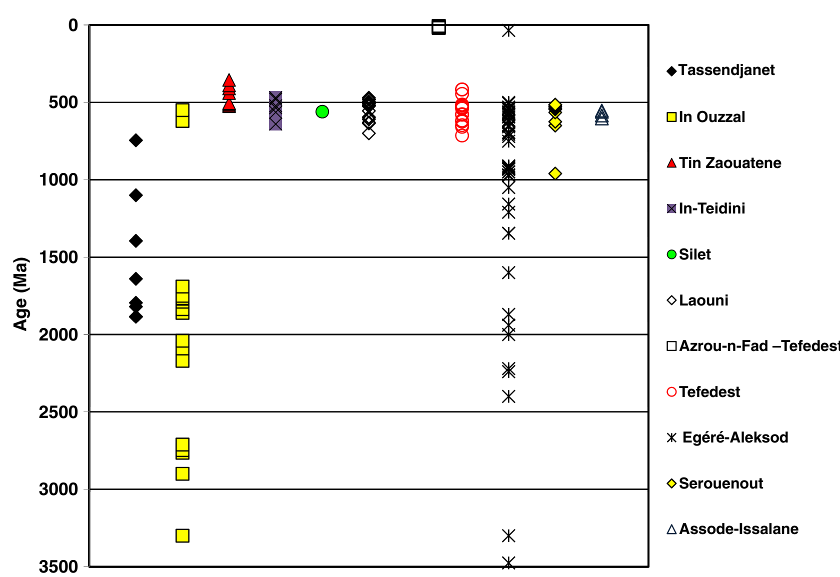

Fig. 2 Distribution of isotopic ages published before 1980, arranged by terranes from west to east

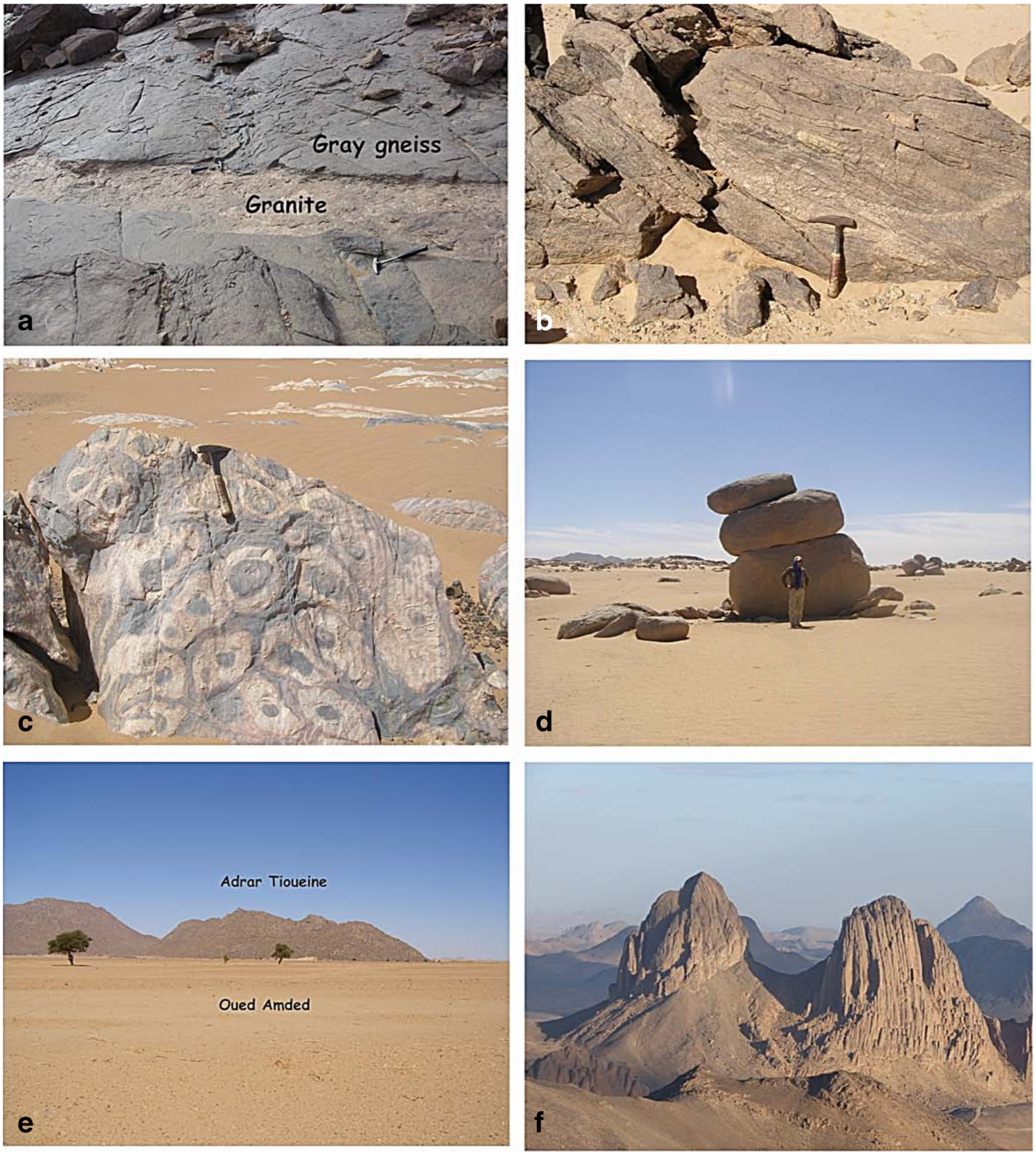

Fig. 3 Field features. **a** Archean. "Série Rouge" grey gneiss cut by a granite dyke (Egere-Aleksod terrane). **b** Paleoproterozoic. Tidjenouine granulitic orthogneiss (Laouni terrane). **c** Neoproterozoic. Timgaouine Conophyton (Silet terrane). **d** Neoproterozoic. Anou-Eheli batholith (Silet terrane). **e** Precambrian-Cambrian boundary. Tioueine Taourirt complex (Silet-In Tedeini terrane boundary). **f** Neogene. Tizouiedj phonolite necks, Atakor volcanic district (Azrou N'Fad terrane). Photographic credits. **a** Nadia Bouregda, **b**–**f**. Faten Bechiri-Benmerzoug

terrane, the Paleoproterozoic is represented exclusively by metamorphic events (2075 ± 30 to 2062 ± 39 Ma) (Bertrand et al. 1986a, b; Bendaoud et al. 2008) (Fig. 3b). Detrital zircons from the Edembo and the Djanet terranes recorded Paleoproterozoic ages from 2438 to 1847 Ma. All Paleoproterozoic ages were recorded in metacratonic areas (Liégeois et al. 2013) and reflect the major role played by the Eburnean orogeny.

The following Mesoproterozoic era corresponds to a long-lasting period of quiescence, referred to as the "boring billion" (Roberts 2013). Neither high-grade metamorphism nor igneous emplacement ages were recorded so far. Yet, as far as the Mesoproterozoic era is concerned, Caby (2003) reported unpublished Pb-Pb ages of 1145–1100 Ma obtained on galena from a stratabound lead occurrence within high-grade Tirek marbles.

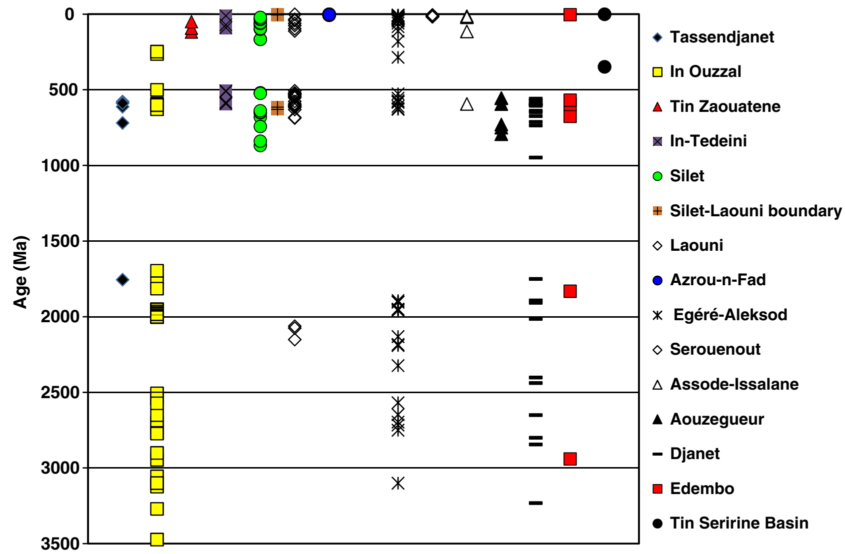

Fig. 4 Diagram of all isotopic ages published after 1980, arranged by terranes from west to east

The Neoproterozoic era is dominant in the geological history of the Hoggar shield (Fig. 7, Table 4). This era is marked by continental crustal growth illustrated by emplacement of a large number of granitoids. In Central Hoggar (Laouni and Egere-Aleksod terranes, parts of the LATEA metacraton), the granitoids intrude garnet-bearing lithologies (eclogite, amphibolite, gneiss). The amphibolite-facies metamorphic events at around 680 Ma accompanied tangential shearing and eclogite obduction (Liégeois et al. 2003). They predated granitoid emplacement at 630 to 550 Ma. The first period between 630 and 600 Ma is characterized by emplacement of the syn-collisional calco-alkaline batholiths, such as Amsel dated at 630 ± 5 and 599 ± 3 Ma (LA-ICP-MS U-Pb zircon, Talmat-Bouzeguela et al. 2011), Anfeg (dated at 615 ± 5 Ma by Bertrand et al. 1986a, b and recalculated at 608 ± 7 Ma by Acef et al. 2003) and subcircular plutons with alkaline affinity as Ounane granodiorite dated at 629 ± 6 Ma (SHRIMP U-Pb zircon, Abdallah et al. 2008). During the second period from 580 to 550 Ma, the post-tectonic batholiths with an alkaline character are dominated as the In Tounin batholiths (LA-ICP-MS U-Pb zircon 552 ± 3 Ma, Abdallah et al. 2011), Tihoudaïne and the Tisselliline granite dated at 580 ± 6 Ma and 572 ± 6 Ma (SHRIMP U-Pb zircon), respectively (Abdallah et al. 2008).

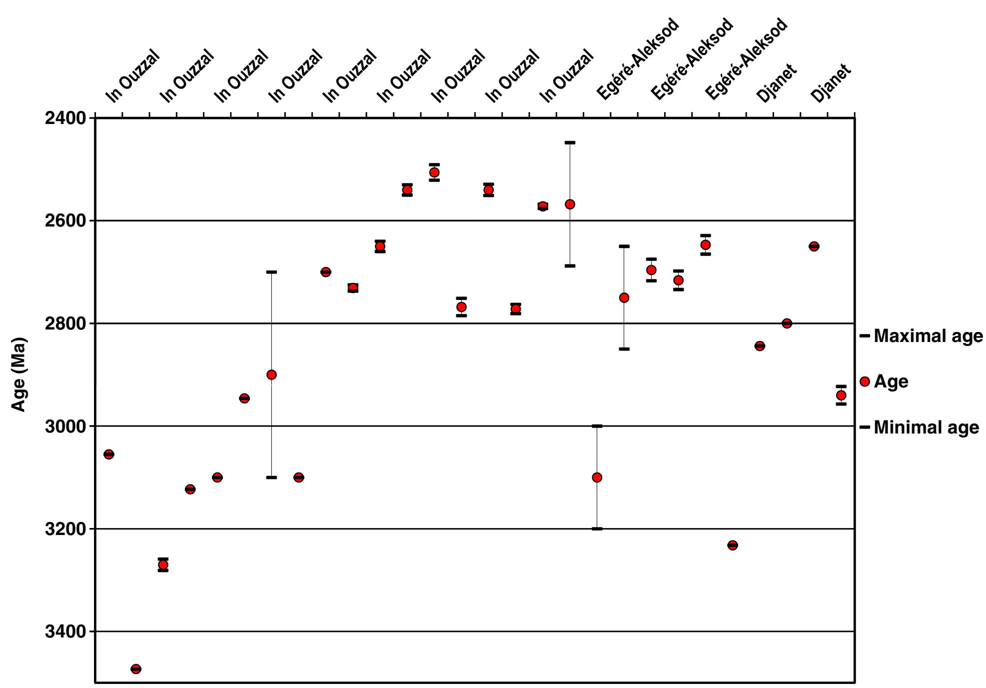

Fig. 5 Distribution of Archaean isotopic ages (with uncertainty) published after 1980, arranged by terranes from west to east

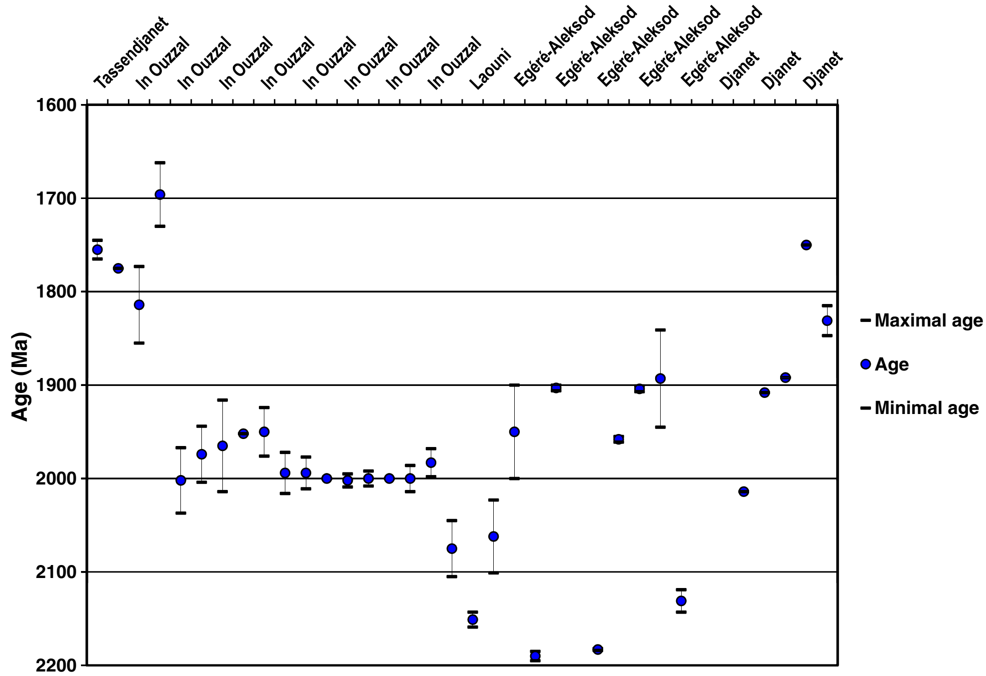

Fig. 6 Distribution of Paleoproterozoic isotopic ages (with uncertainty) published after 1980, arranged by terranes from west to east

In the In-Ouzzal terrane characterized by granulitic basement (Ouzegane et al. 2003), alkali-calcic granitoids were emplaced, like North Tihimatine sub-circular granitic pluton dated at 601 ± 4 Ma (SHRIMP U-Pb zircon) and 600 ± 5 Ma (LA-ICP-MS U-Pb zircon, Fezaa et al. 2011), whereas, in the nearby Tassendjanet terrane, metamorphic events were identified, i.e., 719 ± 7 Ma amphibolite episode within the Ougda volcanic arc and 611 ± 5 to 577 ± 6 Ma HP episodes within the Tidjeridjaouijne belt (^{40}Ar-^{39}Ar amphibole, phengite and biotite; Caby and Monié 2003) coeval with Tin Zebane dyke swarm emplacement (592.2 ± 5.8 Ma, Rb-Sr WR isochron; Hadj Kaddour et al. 1998). In Eastern Hoggar (Edembo terrane), the Ouhot migmatite was metamorphosed and partially melted at 568 ± 4 Ma, coevally to 571–558 Ma alkali-calcic granitic batholiths in the nearby Djanet terrane (Fezaa et al. 2010, Table 4).

Juvenile terranes of the metasediments Pharusian belt (Tin-Zaouatene, In-Tedeini and Silet terranes) are characterized by the occurrence of Neoproterozoic geological formations only. For example, in the Silet terrane (Bechiri-Benmerzoug 2009), numerous granitic batholiths (sodic low-HREE and potassic TTG) were emplaced during the Tonian (three episodes at

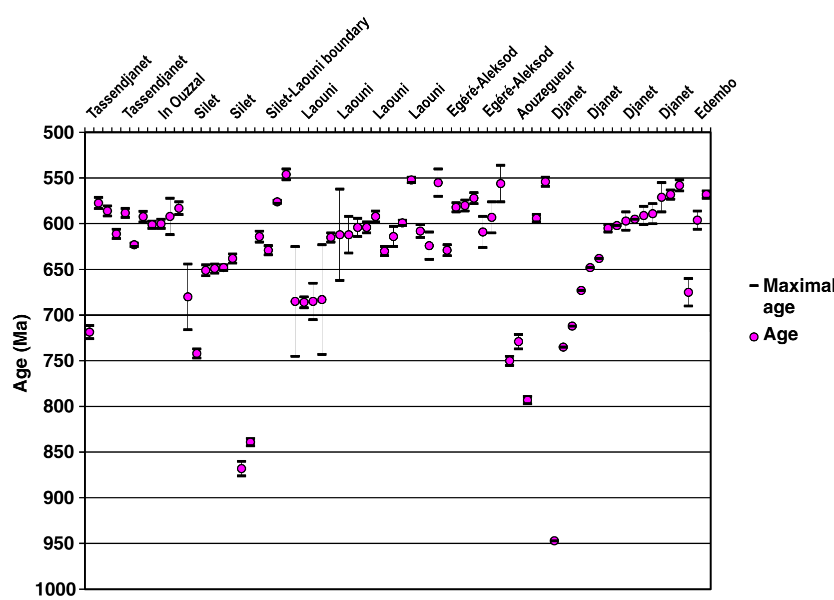

Fig. 7 Distribution of Neoproterozoic isotopic ages (with uncertainty) published after 1980, arranged by terranes from west to east

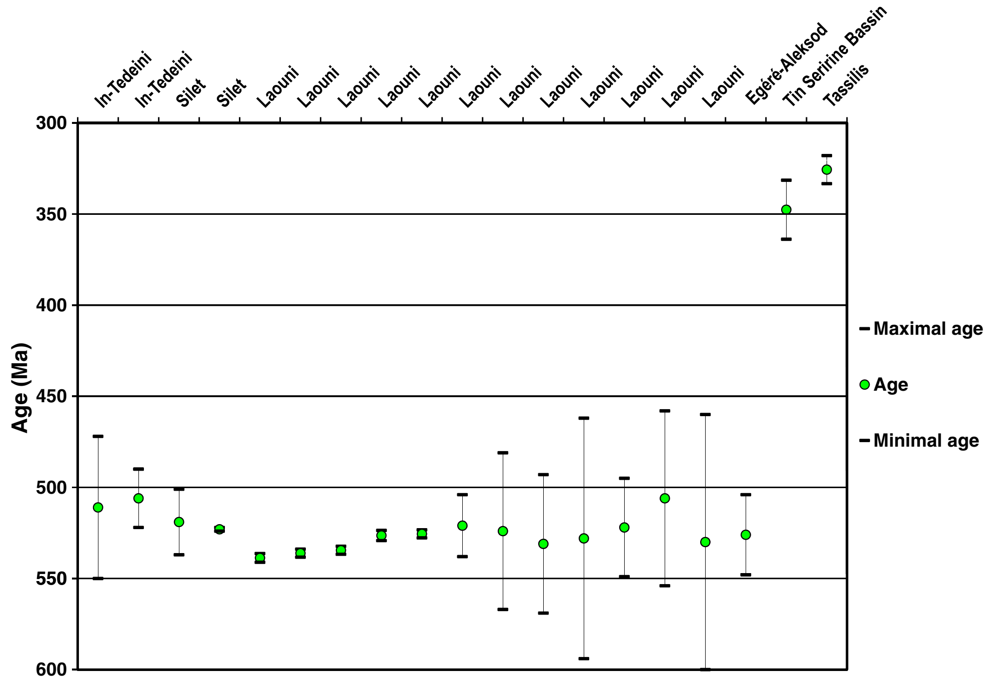

Fig. 8 Distribution of Paleozoic isotopic ages (with uncertainty) published after 1980, arranged by terranes from west to east

868 ± 8, 839 ± 4 and 742 ± 5 Ma, Table 4) and mostly the Cryogenian (tonalite, granodiorite and monzogranite rocks from 651 ± 6 to 638 ± 5 Ma) (Fig. 3c, d). They predate the final collision of the Silet terrane onto the LATEA metacraton (Laouni terrane) at 629 ± 5 Ma (Bertrand et al. 1986a, b). No Ediacaran batholiths were found so far. The Neoproterozoic volcanism which is represented by Irrelouchem volcanic series (basalt, rhyodacite and ignimbrites) exposed in the Tin-Dahar area (Silet terrane) is dated at 680 ± 36 Ma (isochron Rb-Sr WR, Dupont 1987; Table 4).

The Ediacaran period is marked by North-South trending strike-slip shearing episodes, accompanied by emplacement of the Taourirt igneous province. The Taourirt complexes (Azzouni-Sekkal et al. 2003) are composed of alkali-calcic and (per)alkaline A-type granitoids and associated gabbros and alaskites (highly evolved alkali feldspar granites). Their

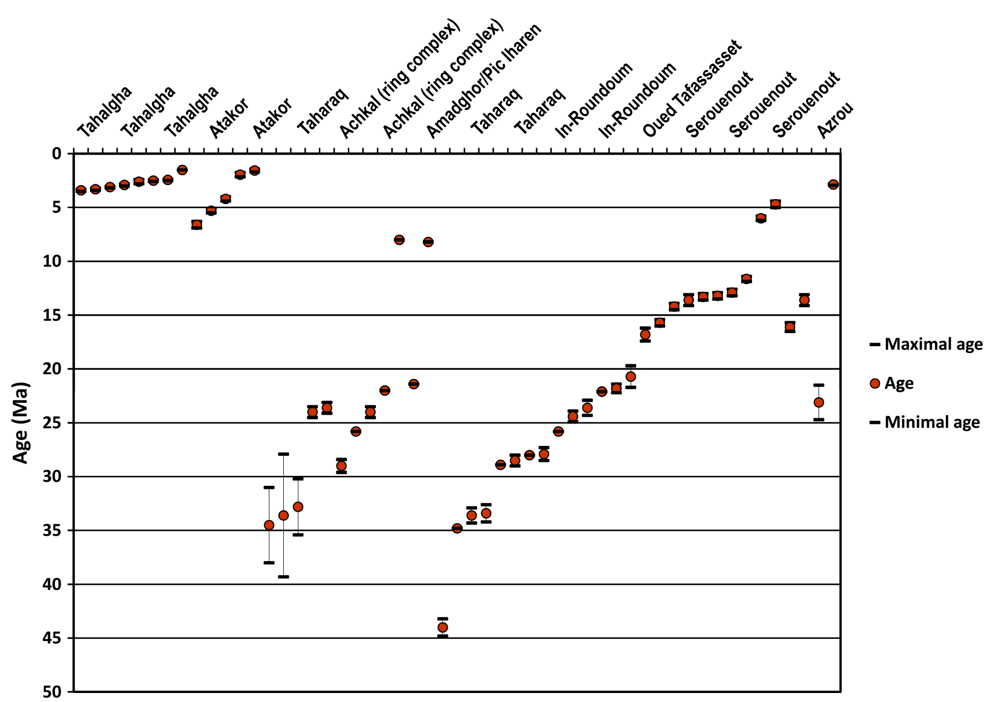

Fig. 9 Distribution of Cenozoic isotopic ages (with uncertainty) published after 1980, arranged by terranes from west to east

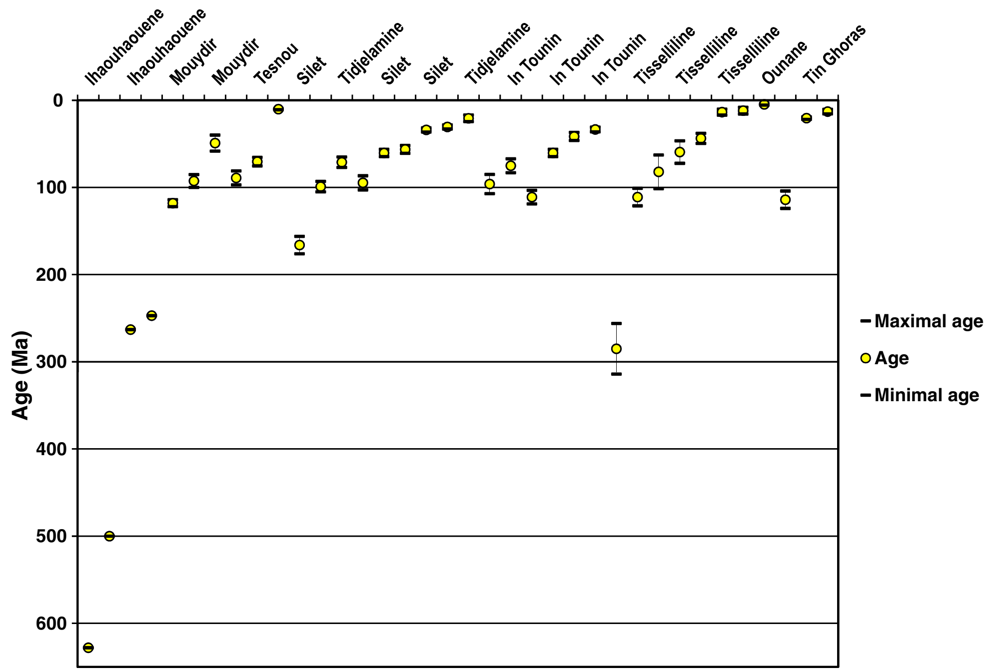

Fig. 10 Distribution of low-temperature thermochronology, arranged by terranes from west to east

emplacement ages are not well-constrained by Cambrian Rb-Sr whole-rock isochrons (Azzouni-Sekkal et al. 2003) and ^{39}Ar-^{40}Ar biotite dates (Cheilletz et al. 1992) ranging from 540 to 505 Ma (Table 5), which may represent late thermal events fostered by strike-slip movements along north-south trending shear zones. For example, the In Tounine Taourirt complex yields 552 ± 3 Ma LA-ICP-MS U-Pb zircon age, interpreted as true emplacement age (Abdallah et al. 2011), 502 ± 42 Ma (Azzouni-Sekkal et al. 2003) or 521 ± 17 Ma (Cheilletz et al. 1992) Rb-Sr whole-rock isochrons, and 535 ± 3 Ma ^{40}Ar-^{39}Ar biotite age (Cheilletz et al. 1992), suggesting that the Taourirt igneous episodes may have occurred mostly during the Ediacaran and that Cambrian ages may reflect either a slow cooling process, or more likely a late-stage hydrothermal event. Yet, the 523 ± 1 Ma U-Pb zircon (TIMS) age on Tioueine alkali feldspar syenite (Paquette et al. 1998) is the only to correspond to late Early Cambrian emplacement (Fig. 3e).

During the Paleozoic era (Fig. 8, Table 5), two major periods were found. In the Early Cambrian, Rb-Sr whole-rock isochrons and ^{39}Ar-^{40}Ar biotite ages on Taourirt complexes, though interpreted formerly as igneous emplacement ages, may actually represent late thermal episodes. Later on, in the southern and eastern Tassili sedimentary cover, the 348 ± 16 Ma (Late Devonian to Early Carboniferous) Tin Serririne dolerite lava (Djellit et al. 2006) and the 326 ± 8 Ma (Serpukhovian) Arrikine gabbroic sill (Derder et al. 2016), measured by ^{40}K-^{40}Ar isotopes on whole-rocks, took part to the widespread Carboniferous igneous events occurring in the nearby North African sedimentary basins.

The Mesozoic era (Table 6) was a period of quiescence in terms of ductile deformation, metamorphic and igneous episodes. During the Cenozoic era (Fig. 9, Table 7), renewed volcanic activity began at ca. 44.0 ± 0.5 Ma, with the outpouring of Taharaq trachybasalt flow followed by a 34.5–24.4 ± 0.5 Ma sequence of tholeiitic flood basalt lava flows (Aït-Hamou et al. 2000). Then, the volcanic activity became more and markedly alkaline in several discrete episodes separated by periods of quiescence. It was active until recent times, with scarce Neolithic artefacts intercalated with lava flows (Benmessaoud 2014). For a more complete review, see Liégeois et al. (2005). The first Late Eocene and Oligocene episodes were confined in the Egere-Aleksod terrane, in the central part of the Hoggar Swell. During Neogene episodes, new districts were formed in between the 4°50′E and the 8°30′E north-south shear zones within the Hoggar Swell, with most of them occupying a diametrical SW-NE trending alignment referred to as the Oued Amded lineament (Aït-Hamou 2006). Discrete episodes are coeval to the successive phases of Africa–Europe convergence (Rougier et al. 2013). Current activity is marked by thermal and/or mineral springs in the south of the Atakor district (for a review of the Atakor volcanic district, see Azzouni-Sekkal et al. 2007) (Fig. 3f). Weak seismic activity, recorded since the 1950s by the Tamanrasset seismological station, occurs near the 4°50′E shear zone, with a recent crisis beginning on May 20th, 2010 (Bourouis et al. 2013; Babkar et al. 2014). It provides ample evidence that, though located within intraplate settings, the Hoggar Swell is not yet stable.

Two studies (Carpena et al. 1988; Rougier 2012) using thermochronological techniques (U-Th/He apatite and zircon, apatite fission tracks) were made to unravel exhumation mechanics of the Hoggar Swell (Fig. 10, Tables 5 to 7). Discrete low-temperature episodes affected Paleoproterozoic carbonatites in the In-Ouzzal terrane during the Pan-African orogeny and, afterwards, during the final stage of the Variscan orogeny, as emphasized by Ediacaran (628 Ma), Mid-Cambrian (500 Ma) and, later on, Mid-Permian (263 Ma) apatite fission track ages (Carpena et al. 1988). Elsewhere, apatite fission tracks and U-Th/He ages spread from the Early Permian (285 Ma) to the Pliocene (5 Ma) (Rougier et al. 2013). Cretaceous sedimentary remnants at high elevations suggest subsidence during the Mesozoic, with burial of more than 1 km after the Early Cretaceous. Thermal models reflecting large-scale vertical processes demonstrate widespread Eocene exhumation of the entire shield before volcanic activity began in the Late Eocene (Rougier et al. 2013).

Summary and concluding remarks

Increasingly precise isotopic dating techniques illustrate the protracted geological history of the Hoggar Shield.

The first continental *nuclei* were formed in the Archean era. A second series of continental terranes were created during the Paleoproterozoic Eburnean orogeny. A long-lasting period of quiescence, referred to as the "boring billion", corresponds to cratonization processes in the Mesoproterozoic.

Cratonic to metacratonic terranes were reworked and accompanied juvenile terranes during the Neoproterozoic–Lower Paleozoic Pan-African orogeny. At the final stages of the orogeny, the Hoggar Shield acquired its definitive shape defined by strike-slip movements along north-south-trending shear zones.

After scarce Carboniferous emplacement of mafic magmatic formations, the Mesozoic and the beginning of the Cenozoic are again a long period of quiescence, with neither high-grade metamorphism, nor igneous emplacements. Widespread Eocene exhumation predated the Late Eocene to recent volcanic activity.

Low-temperature thermochronological ages show Mesozoic subsidence, with burial up to 1 km after the Early Cretaceous, followed by Eocene exhumation giving to the Hoggar its current landscape.

Comparison of the different dating techniques indicates that emplacement ages of magmatic formations and/or protoliths of orthogneisses should be measured by U-Pb zircon ages, whereas the other techniques show only late-stage hydrothermal processes, except K-Ar techniques for Cenozoic volcanic formations. Thus, new U-Pb zircon ages are warranted in order to get more precisely dated geological episodes.

Acknowledgments The age dataset was acquired using classical search engines. In addition, we wish to thank warmly the colleagues having worked, or still working, on Hoggar geology. They were particularly helpful in the determination and the discussion of various aspects of Hoggar geological history. Among them, we are especially indebted to the late Russell Black, Jean-Michel Bertrand, Louis Latouche, Maurice Lelubre and Pierre Rognon, as well as to Jean Boissonnas, Renaud Caby, Michel Gravelle, Jean-Robert Kienast, Jean-Paul Liégeois, Georges Vitel, Abla Azzouni-Sekkal, Khadidja Ouzegane, Aziouz Ouabadi and the teams of ORGM's geologists. Thorough reviews by anonymous reviewers are gratefully acknowledged.

References

Abbassene F, Oubadi A (2010) Pétrologie et géochimie du massif granitique Pan-africain d'Arif (Terrane d'Aouzegueur, Hoggar Oriental, Algérie). In: Proceedings Geomag 1, Tlemcen, Algérie, 10–12 November, pp 12–15

Abdallah N, Liégeois JP, De Waele B, Fezaa N, Ouabadi A (2007) The Temaguessine Fe-cordierite orbicular granite (Central Hoggar, Algeria): U–Pb SHRIMP age, petrology, origin and geodynamical consequences for the late Pan-African magmatism of the Tuareg shield. J Afr Earth Sci 49:153–178

Abdallah N (2008) Géochimie et Géochronologie des intrusions magmatiques panafricaines du terrane Egéré-Aleksod : exemple des massifs granitiques de l'Ounane, Tihoudaîne et Tisselliline (Hoggar central, Algérie) Thèse Doctorat (USTHB/FSTGAT) Algérie, 201pp

Abdallah N, Liégeois JP, Boissonnas J, De Waele, B, Fezaa N, Ouabadi A (2011) In Tounine: a Murzukian-related pluton in LATEA (Tuareg Shield, Algeria). 23rd Colloquium of African Geology (Cag 23), Abstract volume, University of Johannesburg, South Africa, 8–14 January, 1

Abdelsalam MG, Liégeois JP, Stern RJ (2002) Saharan Metacraton. J Afr Earth Sci 34(3–4):119–136

Acef K, Liégeois JP, Ouabadi A, Latouche L (2003) The Anfeg post-collisional Pan-African high-K calc-alkaline batholith (Central Hoggar, Algeria), result of the LATEA microcontinent metacratonization. J Afr Earth Sci 37:295–311

Adjerid Z, Godard G, Ouzegane K (2015) High-pressure whiteschists from the Ti-N-Eggoleh area (Central Hoggar, Algeria): a record of Pan-African oceanic subduction. Lithos 226:201–216

Aït-Hamou F (2000) Thèse de doctorat en sciences. In: Un exemple de "point chaud" intra-continental en contexte de plaque quasistationnaire: Étude pétrologique et géochimique du Djebel Taharaq et évolution du volcanisme cénozoïque de l'Ahaggar (Sahara Algérien). Université de Montpellier II–Sciences et Techniques du Languedoc, Montpellier, France, p 200

Aït-Hamou F (2006) Le Volcanisme Cénozoïque à l'échelle du bombement de l'Ahaggar (Sahara Central Algérien) : synthèse géochronologique et répartition spatio-temporelle. Quelques implications en relation avec l'histoire Eo-alpine de la plaque afrique. Mém. Serv. Géol. Nation. no 13, 2 fig., 2 tabl., pp. 155–167

Aït-Hamou F, Dautria JM (1994) Le magmatisme cénozoïque du Hoggar: Une synthèse des données disponibles: Mise au point sur l'hypothèse d'un point chaud. Bull Serv Géol Algér 5:49–68

Aït-Hamou F, Dautria JM, Cantagrel JM, Dostal J, Briqueu L (2000) Nouvelles données géochronologiques et isotopiques sur le volcanisme cénozoïque de l'Ahaggar (Sahara algérien): Des arguments en faveur d'un panache. C R Acad Sci Paris, v. 330, pp. 829–836

Allègre CJ, Caby R (1972) Chronologie absolue du Precambrien de l'Ahaggar occidental. C.R. somm. Soc. Geol., v. 275, p. 2095–2098

Allegre CJ, Dupré B, Lambert B, Richard P (1981) The subcontinental versus the sub-oceanic debate—I. Lead-neodymium-strontium isotopes in primary alkali basalts from a shield area: the Ahaggar volcanic suite. Earth Planet Sci Lett 52:85–92

Arab A, Ouzegane K, Drareni A, Doukkari S, Zetoutou S, Kienast JP (2015) Phase equilibria modeling of kyanite-bearing eclogitic metapelites in the NCKFMASHTO system from the Egere terrane (Central Hoggar, South Algeria) Arab J Geosci, 8–5, pp 2443–2455

Ayadi A, Dorbath C, Lesquerd A, Bezzeghouda M (2000) Crustal and upper mantle velocity structure of the Hoggar swell (Central Sahara, Algeria). Phys Earth Planet Inter 118(1–2):111–123

Azzouni-Sekkal A, Liégeois J-P, Bechiri-Benmerzoug F, Belaidi-Zinet S, Bonin B (2003) The “Taourirt” magmatic province, a marker of the closing stage of the Pan-African orogeny in the Tuareg shield: review of available data and Sr–Nd isotope evidence. J Afr Earth Sci 37:331–350

Azzouni-Sekkal A, Bonin B, Benhallou A, Yahiaoui R, Liégeois JP (2007) Cenozoic alkaline volcanism of the Atakor massif, Hoggar, Algeria. In: Beccaluva L et al (eds) Cenozoic volcanism in the Mediterranean area: Geological Society of America Special Paper, vol 418, pp 321–340

Babkar Y, Yelles-Chaouche A, Benhallou AZ, Bendekken A, Hacini AO, (2014) Étude du séisme de Tamanrasset du 14 février 2013 dans le contexte de la sismicité du Hoggar. Colloque Géologie et Ressources Minérales du Hoggar, Alger, 9–13 Novembre 2014, poster

Barbey P, Bertrand JM, Angoua S, Dautel D (1989) Petrology and U/Pb geochronology of the Telohat migmatites, Aleksod, central Hoggar, Algeria. Contrib Mineral Petrol 101:207–219

Bechiri-Benmerzoug F (2009) Pétrologie, géochimie isotopique et géochronologie des granitoïdes Pan-africains de type TTG de Sielt: contribution à la connaissance de la structuration du bloc d’Iskel (Silet, Hoggar occidental) Algérie, thèse de Doctorat (USTHB/FSTGAT) Algérie, 335 p

Bechiri-Benmerzoug F, Liégeois JP, Bonin B, Azzouni-Sekkal A, Bechiri H, Kheloui R, Matukov DI, Sergeev SA (2011) The plutons from the Cryogenian Iskel composite oceanic island arc (Hoggar, Tuareg Shield, Algeria): U–Pb on zircon SHRIMP geochronology, geochemistry and geodynamical setting. Seventh Hutton Symposium on Granites and Related Rocks, Avila, Spain, July 4–9 2011, p. 17

Ben El Khaznadji R, Azzouni-Sekkal A, Benhallou A, Liégeois JP, Bernard B (2017) Neogene felsic volcanic rocks in the Hoggar province: volcanology, geochemistry and age of the Azrou trachyte-phonolite association (Algerian Sahara). J Afr Earth Sci 127:222–234

Ben Othmane D, Polvé M, Allègre CJ (1984) Nd-Sr isotopic composition of granulites and constraints on the evolution of the lower continental crust. Nature 307:512–515

Bendaoud A, Ouzegane K, Godard G, Liégeois JP, Kienast JR, Bruguier O, Drareni A (2008) Geochronology and metamorphic P–T–X evolution of the Eburnean granulite facies metapelites of Tidjenouine (Central Hoggar, Algeria): witness of the LATEA metacratonic evolution. In: Ennih, N., Liégeois, J.P. (Eds.), The boundaries of the West African Craton. Geological Society, London, Special Publications, 297, pp. 111–146

Benmessaoud M (2014) Recherches sur l’Acheuléen de l’Ahaggar. Les matières premières lithiques; l’outillage lithique, rapport éclats/outil; le cadre stratigraphique et chronologique. “Exemple du site Téhéntawek”. Thèse de doctorat en archéologie. Université de Paris 1, Panthéon-Sorbonne, 206 p

Berger J, Ouzegane K, Bendaoud A, Liégeois JP, Kienast JR, Bruguier O, Caby R (2014) Continental subduction recorded by Neoproterozoic eclogite and garnet amphibolites from Western Hoggar (Tassendjanet terrane, Tuareg Shield, Algeria). Precambrian Res 247:139–158

Bernard-Griffiths J, Peucat JJ, Fourcade S, Kienast JR, Ouzegane K (1988) Origin and evolution of 2 Ga old carbonatite complex (Ihouhaouene, Ahaggar, Algeria): Nd and Sr isotopic evidence. Contrib Mineral Petrol 100:339–348

Bertrand JML, Caby R (1978) Geodynamic evolution of the Pan-African orogenic belt: a new interpretation of the Hoggar shield. Geol Rundsch 67:357–388

Bertrand JML, Lassere M (1976) Panafrican and Precambrian history of the Hoggar (Algerian Sahara) in the light of new geochronogical data from the Aleksod area. Precambrian Res 3:343–362

Bertrand JML, Lasserre M (1973) Âge éburnéen de la série de l'Arechchoum (Hoggar central, Sahara algérien). C R Acad Sci 276:1657–1660

Bertrand JML, Boissonnas J, Caby R, Gravelle M, Lelubre M (1966) Existence d’une discordance dans l’antécambrien du “fossé” pharusien de l’Ahaggar occidental (Sahara central). C R Acad Sc Paris 262(D):2197–2200

Bertrand JML, Cantagrel JM, Lasserre M (1972) Age K/Ar mesuré sur des amphiboles dans le Précambrien de l'Aleksod (Ahaggar centra-oriental, Sahara algérien). C R Acad Sci Paris, D 274:1881–1884

Bertrand JML, Caby R, Ducrot J, Lancelot J, Moussine-Pouchkine A, Saadallah A (1978) The late Pan-African intracontinental fold belt of the Eastern Hoggar (central Sahara, Algeria): geology, structural development, U/Pb geochronology, tectonic implications for the Hoggar shield. Precambrian Res 7:349–376

Bertrand JML, Meriem D, Lapique F, Michard A, Dautel D, Ravelle M (1986a) Nouvelles données sur l’âge de la tectonique pan-africaine dans le rameau oriental de la chaîne pharusienne (région de Timgaouine, Hoggar, Algérie). C R Acad Sci Paris 302:437–440

Bertrand JML, Michard A, Boullier AM, Dautel D (1986b) Structure and U/Pb geochronology of Central Hoggar (Algeria): a reappraisal of its Pan-African evolution. Tectonics 5:955–972

Black R, Latouche L, Liégeois JP, Caby R, Bertrand JM (1994) Pan-African displaced terranes in the Tuareg shield (Central Sahara). Geology 22:641–644

Boissonnas J (1969) Nouvelles précisions sur les granites post-tectoniques de la région de Tamanrasset (Sahara central, Algérie). C R Acad Sci Paris, D 268:1909–1911

Boissonnas J, Duplan L, Maisonneuve J, Vachette M, Vialette Y (1964) Étude géologique et géochronologique des roches du compartiment suggarien du Hoggar central (Algérie). Ann Fac Sci, Univ Clermont-Ferrand 25(8):73–90

Boissonnas J, Borsi S, Ferrara G, Fabre J, Fabries J, Gravelle M (1969) On the Early Cambrian age of two late-orogenic granites from west-central Ahaggar (Algerian Sahara). Can J Earth Sci 6:25–27

Boissonnas J, Leutwein F, Sonet J (1970) Age du granite hyperalcalin de la Gara Adjemamaye (Ahaggar du Sud-Est, Sahara algérien). CR Somm Soc Géol Fr 7:251–252

Boissonnas J (2008) Cisaillements ductiles et mise en place de plutons granitiques dans le nord de la chaîne panafricaine du Sahara central : le secteur de Tinnirt (Mouydir, Hoggar du NW, Algérie). Bulletin du Service Géologique National, 19(2), pp. 101–113.

Boughrara M (1999) Thèse de doctorat. In: Analyse pétrologique et géochronologique de la région de Tin Begane (Hoggar, Algérie): un exemple de la datation d’une série métamorphique en contexte polycyclique. MNHN, Paris, France, p 198

Bourouis S, Sebai A, Akacem M, Yelles-Chaouche AK (2013) Intraplate seismicity of the Hoggar region (South Algeria). ESC, poster

Briedj M (1993) Etude géologique de la région de Tahifet (Hoggar Central, Algérie). Implications géodynamiques. Thèse Doctorat. Université Nancy I, 200p.

Caby R (2003) Terrane assembly and geodynamic evolution of central–western Hoggar: a synthesis. J Afr Earth Sci 37:133–159

Caby R, Andreopoulos-Renaud U (1983) Age à 1800 Ma du magmatisme sub-alcalin associé aux métasédiments monocycliques de la chaîne panafricaine du Sahara central. J Afr Earth Sci 1:193–197

Caby R, Andreopoulos-Renaud U (1987) Le Hoggar oriental, bloc cratonisé à 730 Ma dans la chaîne pan-africaine du nord du continent africain. Precambrian Res 36:335–344

Caby R, Monié P (2003) Neoproterozoic subduction and differential exhumation of western Hoggar (southwest Algeria): new structural, petrological and geochronological evidence. J Afr Earth Sci 37: 133–159

Caby R, Andreopoulos-Renaud U, Gravelle M (1982) Cadre géologique et géochronologie U/Pb sur zircon des batholites précoces dans le segment panafricain du Hoggar central (Algérie). Bull Soc Géol Fr 7:876–882

Cahen L, Snelling NJ, Delhal J, Vail JR, Bonhomme M, Ledent D (1984) The geochronology and evolution of Africa. Clarendon Press, Oxford 508 p

Carpena J, Kienast JR, Ouzegane K, Jehanno C (1988) Evidence of the contrasted fission-track clock behavior of the apatites from In Ouzzal carbonatites (northwest Hoggar): The low-temperature thermal history of an Archean basement. Geol Soc Am Bull, v. 100, pp. 1237–1243

Cheilletz A, Bertrand JM, Charoy B, Moulahoum O, Bouabsa L, Farrar E, Zimmerman JL, Dautel D, Archibald DA, Boullier AM (1992) Géochimie et géochronologie Rb–Sr, K–Ar et ^{39}Ar–^{40}Ar des complexes granitiques pan-africains de la région de Tamanrasset (Algérie): relations avec les minéralisations Sn–W associées et l'évolution tectonique du Hoggar central. Bull Soc Géol Fr 163: 733–750

Derder MEM, Maouche S, Liégeois JP, Henry B, Amenna M, Ouabadi A, Bellon H, Bruguier O, Bayou B, Bestandji R, Nouar O, Bouabdallah H, Ayache M, Beddiaf M (2016) Discovery of a Devonian mafic magmatism on the western border of the Murzuq basin (Saharan metacraton): paleomagnetic dating and geodynamical implications. J Afr Earth Sci 115:159–176

Djellit H, Bellon H, Ouabadi A, Derder M, Henry B, Bayou B, Khaldi A, Baziz K, Merahi M (2006) Âge $^{40}K/^{40}Ar$, Carbonifère inférieur, du magmatisme basique filonien du synclinal paléozoïque de Tin Serririne, Sud-Est du Hoggar (Algérie). Compt Rendus Geosci 338:624–631

Dostal J, Keppie JD, Cousens BL, Murphy JB (1996) 550–580 Ma magmatism in Cape Breton Island, 5Nova Scotia, Canada: the product of NW-dipping subduction during the final stage of assembly of Gondwana. Precambrian Res 76:96–113

Doukkari SA, Ouzegane K, Arab A, Kienast JR, Godard G, Drareni A, Zetoutou S, Liégeois JP (2014) Phase relationships and P–T path in NCFMASHTO system of the eclogite from the Tighsi area (Egere terrane, Central Hoggar, Algeria). J Afr Earth Sci 99:276–286

Doukkari, S.A, Ouzegane K, Godard G, F.A. Diener, J., Jean-Robert Kienast,J-P Liégeois, A Arab, A Drareni (2015) Prograde and retrograde evolution of eclogite from Adrar Izzilatène (Egéré-Aleksod terrane, Hoggar, Algeria) determined from chemical zoning and pseudosections, with geodynamic implications. Lithos 226. 217–232

Drareni A, Ouzegane K, Bendaoud A (2007) L'Archéen du Hoggar: géochronologie et évolution géodynamique. Bull Serv Géol Algér 18:103–126

Dupont PL (1987) Implications géodynamiques pour l'évolution d'une chaîne mobile au Protérozoïque supérieur. In: Pétrologie et géochimie des ensembles magmatiques Pharusien I et Pharusien II dans le rameau oriental de la chaîne pharusienne (Hoggar, Algérie). Thèse Doctorat, Université de Nancy I, France, p 283

Eberhardt P, Ferrara G, Glangeaud L, Gravelle M, Tongiorgi E (1963) Sur l'âge absolu des séries métamorphiques de l'Ahaggar occidental dans la région de Silet-tibehaouine (Sahara central). C R Acad Sci 256: 1126–1128

Ferrara G, Gravelle M (1966) Radiometric ages from Western Ahaggar (Sahara) suggesting an eastern limit for the West African Craton. Earth Planet Sci Lett 1:319–324

Fezaa N, Liégeois JP, Abdallah N, Cherfouh EH, De Waele B, Bruguier O, Ouabadi A (2010) Late Ediacaran geological evolution (575–555 Ma) of the Djanet Terrane, Eastern Hoggar, Algeria, evidence for a Murzukian intracontinental episode. Precambrian Res 180: 299–327

Fezaa N, Liégeois JP, Abdallah N, De Waele B, Bruguier, and Ouabadi, A. (2011) The Pan-African Granites in the Archean In Ouzzal metacraton (Hoggar, Algeria). 23rd Colloquium of African Geology (Cag23), Abstracts Volume, University of Johannesburg, South Africa, 8–14 January, 143

Gautier EF (1908) Mission au Sahara algérien, Paris, Armand Colin, 2 vol. in-8, pp 371

Gautier EF (1928) Le Sahara, Paris Payot., in-8, pp 232

Girod M (1971) Le massif volcanique de l'Atakor (Hoggar, Sahara Algérien). Etude pétrographique, structurale et volcanologique. Mémoires CRZA n°12, série géologie. CNRS editions, Paris, 1 vol., 158 p

Guérangé B, Lasserre M (1971) Étude géochronologique de roches du Hoggar oriental par la méthode au strontium. CR Somm Soc Géol Fr 4:213–215

Haddoum H, Mokri M, Ouzegane K, Aït Djaffer S, Djemai S (2013) Extrusion de l'In Ouzzal vers le Nord (Hoggar occidental, Algérie): une conséquence d'un poinçonnement panafricain. J Hydrocarb Min Environ Res 4(1):6–16

Hadj Kaddour Z, Demaiffe D, Liégeois JP, Caby R (1998) The alkaline–peralkaline granitic post-collisional tin Zebane dyke swarm (Pan-African Tuareg shield, Algeria): prevalent mantle signature and late agpaitic differentiation. Lithos 45:223–243

Hellal B (1987) Etude pétrographique et géochronologique d'une quartzite ferrifère de l'archéen du bouclier Touareg (In Ouzzal, Algérie). D.E.A, Université Paris VI, France 76 p

Henry B, Liégeois JP, Nouar O, Derder MEM, Bayou B, Bruguier O, Ouabadi A, Belhai D, Amenna M, Hemmi A, Ayache M (2009) Repeated granitoid intrusions during the Neoproterozoic along the western boundary of the Saharan metacraton, eastern Hoggar, Tuareg shield, Algeria: an AMS and U–Pb zircon age study. Tectonophysics 474:417–434

Kahoui M, Liégeois JP, Mahdjoub Y, Louni C (2011) Post-collisional alkaline magmatism in the Gara Adjemamaye area (Hoggar, Algeria). In: 23rd Colloquium of African Geology (Cag23), vol Abstracts Volume. University of Johannesburg, South Africa, pp 8–14

Karpoff R (1946) Le Nigritien de l'Adrar Tira 'rar (Adrar de Iforas, Sahara). CR Acad Sci 233:428–429

Kilian C (1947) Du Précambrien d'Afrique. CR Somm Soc Géol Fr 224: 350–352

Killian C (1924) Notes sur la géologie du Sahara central. Géol Alp 13:87–102

Killian C (1932) Sur des conglomérats précambriens du Sahara central. CR Somm Soc Géol Fr 4:87

Lancelot JR, Vitrac A, Allegre CJ (1976) Uranium and lead isotopic dGéologique ating with grain-by-grain zircon analysis: a study of complex geological history with a single rock. Earth Planet Sci Lett 29:357–366

Latouche L, (1978) Etude pétrographique et structurale du Précambrien de la région des Gour Oumelalen (NE Hoggar, Algérie). Thèse Doc. Etat. Univ. Paris VII, 225 p

Latouche L, Vidal P (1974) Géochronologie du Précambrien de la région des Gour oumlalen (NE de l'Ahaggar, Algérie). Un exemple de mobilisation du strontium radiogénique. Bull Soc Géol Fr XVI: 195–203

Lay C, Ledent D (1963) Mesures d'âges absolus de minéraux et de roches du Hoggar (Sahara central). CR Acad Sci Paris 257:3188–3191

Lay C, Ledent D, Grögler (1965) Mesures d'âges absolus de zircons du Hoggar (Sahara central). CR Acad Sci Paris 260:3113–3115

Lelubre M (1951) Conrad Kilian (1898–1950). Trav Inst Rech Sahariennes, Alger 7:15–21

Lelubre M (1952) Recherches sur la géologie de l'Ahaggar central et occidental (Sahara central). Bull Serv Géol Algér 22:tome 1, 354–tome 2, 387

Liégeois JP, Black R, Navez J, Latouche L (1994) Early and late Pan-African orogenies in the Aïr assembly of terranes (Tuareg shield, Niger). Precambrian Res. v. 67, pp. 59–66

Liégeois JP, Latouche L, Boughrara M, Navez J, Guiraud M (2003) The LATEA metacraton (Central Hoggar, Tuareg shield, Algeria): behaviour of an old passive margin during the Pan-African orogeny. J Afr Earth Sci 37:161–190

Liégeois JP, Benhallou A, Azzouni-Sekkal A, Yahiaoui R, Bonin B, (2005) The Hoggar swell and volcanism: reactivation of the Precambrian Tuareg shield during Alpine convergence and West African Cenozoic volcanism. In: Foulger, GR, Natland, JH, Presnall, DC, Anderson, DL (Eds), Plates, plumes and paradigms Geol Soc America Spec, Paper, vol. 388, pp. 379–400

Liégeois JP, Abdelsalam MG, Ennih N, Ouabadi A (2013) Metacraton: nature, genesis and behavior: Gondwana Res. v. 23, pp. 220–237

Ludwig KR (1991) Isoplot—a plotting and regression program for radiogenic isotope data. USGS Open-File report, pp91–445

Ludwig KR (2012) Isoplot 3.75, a geochronological toolkit for Excel. 5. Berkeley Geochronology Center Special, Publication, p. 75

Maluski H, Monié P, Kienast JR, Rahmani A (1990) Location of extraneous argon in granulitic-facies minerals: a paired micropobe-laser $^{40}Ar/^{39}Ar$ analysis. Chem Geol 80:213–217

Maza M, Dautria JM, Briqueu L, Cantagrel JM (1995) Massif annulaire de l'Achkal: Un témoin d'un magmatisme alcalin d'âge oligocène supérieur au Hoggar centro-oriental. Bull Serv Géol Algér 6:61–77

Maza M, Briqueu L, Dautria JM, Bosch D (1998) The Achkal Oligocene ring complex: Sr, Nd, Pb evidence for transition between tholeitic and alkali cenozoic magmatism in central Hoggar (South Algeria). Comptes Rendus de l'Académie des Sciences. Paris- série IIa 327, 167–172.

Ouzegane K, Kienast JR, Bendaoud A, Drareni A (2003) A review of Archaean and Paleoproterozoic evolution of the In Ouzzal granulitic terrane (Western Hoggar, Algeria). J Afr Earth Sci 37:207–227

Paquette JL, Caby R, Djouadi MT, Bouchez JL (1998) U–Pb dating of the end of Pan-African orogeny in the Tuareg shield: the post-collisional syn-shear Tioueine pluton (Western Hoggar, Algeria). Lithos 45: 245–253

Peucat JJ, Capdevila R, Drareni A, Choukroune P, Fanning M, Bernard-Griffiths J, Fourcade S (1996) Major and trace element geochemistry and isotope (Sr, Nd, Pb, O) systematics of an Archaean basement involved in a 2.0 Ga VHT (1000°C) metamorphic event: In Ouzzal massif, Hoggar, Algeria. J Metamorph Geol 14:667–692

Peucat JJ, Drareni A, Latouche L, Deloule E, Vidal P (2003) U–Pb zircon (TIMS and SIMS) and Sm–Nd whole rock geochronology of the Gour Oumalelen granulitic basement, Hoggar massif, Tuareg shield, Algeria. J Afr Earth Sci 37:229–239

Roberts NMW (2013) The boring billion?—Lid tectonics, continental growth and environmental change associated with the Columbia supercontinent. Geosci Front 4:681–691

Rossi PL, Lucchini F Savelli C (1979) Données géologiques et radiométriques sur la mise en place de la Tellerteba (Hoggar). 10° Colloque de Géologie Africaine, Montpellier, France, p. 143

Rougier S (2012) Interactions lithosphère–asthénosphère et mouvements verticaux: le cas du massif du Hoggar, Thèse de Doctorat, université paris-sud (Orsay), pp 276

Rougier S, Missenard Y, Gautheron C, Barbarand J, Zeyen H, Pinna R, Liégeois JP, Bonin B, Ouabadi A, El-Messaoud M, Derder MEM, Frizon de Lamotte D (2013) Eocene exhumation of the Tuareg Shield (Sahara Desert, Africa). Geology 41(N°05):615–618 Geological Society of America

Talmat-Bouzeguela S, Liégeois JP, Bruguier O, Ouabadi A (2011) The Pan-African Amsel batholith and the Latea metacratonization (Hoggar, Algeria). 23rd Colloquium of African Geology (Cag23), vol Abstracts Volume. University of Johannesburg, South Africa 8–14 January, p. 378

Vialette Y, Vitel G (1979) Geochronological data on the Amsianassene Tefedest block (Central "Hoggar", Algerian Sahara) and evidence for its polycyclic evolution. Precambrian Res 9:241–254

Yahiaoui R, Dautria JM, Alard O, Bosch D, Azzouni-Sekkal A, Bodinier JL (2014) A volcanic district between the Hoggar uplift and the Tenere Rifts: volcanology, geochemistry and age of the In-Ezzane lavas (Algerian Sahara). J Afr Earth Sci 92:14–20

Zeghouane H (2006) Pétrologie, géochimie, géochimie isotopique et géochronologie Rb/Sr du massif granitique d'Arirer (terrane Aouzegueur, Hoggar oriental) Algérie. Thèse Magister, USTHB, Alger, Algérie. 118 p

Zetoutou S, Ouzegane K, Boubazine S, Kienast JR (2004) Azrou N' Fad (central Hoggar, Algeria) one of the deepest terranes of LATEA: arguments based on P–T evolution in eclogites. J Afr Earth Sci 39: 193–220